2017

Zebrafish (Danio rerio) as a Model for Orofacial Research

Kevin A. Ghaffari

College of Humanities and Sciences

Virginia Commonwealth University

This is to certify that the thesis prepared by Kevin Amir Ghaffari entitled Zebrafish (*Danio rerio*) as a Model for Orofacial Research has been approved by his committee as satisfactory completion of the thesis requirements for the degree of Master of Science.

Robert M. Tombes, Ph.D., Vice Provost, Life Sciences

Sarah Rothschild, Ph.D., Department of Biology

René Olivares-Navarrete, D.D.S., Ph.D., School of Engineering

---

James Lister, Ph.D., Department of Human and Molecular Genetics

---

Date

Zebrafish (*Danio rerio*) as a Model for Orofacial Research

A thesis submitted in partial fulfillment of the requirements for the degree of

Master of Science at Virginia Commonwealth University

By

Kevin Amir Ghaffari

B.S. Virginia Commonwealth University, 2015

Mentor

Robert M. Tombes, Ph.D.

Vice Provost, Life Sciences

Virginia Commonwealth University

Richmond Virginia

April 2017

Acknowledgements

I would like to thank Dr. Robert M. Tombes for everything he has done for me over the past 4 years I have had the pleasure of knowing him. Not only has he been an amazing mentor, motivator, and professional but he has also been a great friend. I will always cherish the experience I have had working with him as a master's student, personal trainer, and preceptor. I would also like to thank Dr. Sarah Rothschild for her absolutely phenomenal mentoring during the course of my master's degree. Her bountiful knowledge can only be overshadowed by her incredible work ethic – a trait I found to be incredibly inspiring throughout my time as a master's student. Furthermore, I would like to thank my remaining committee members, Dr. Olivares-Navarrete and Dr. Lister for their encouragement, suggestions and support. I would like to thank my amazing coworkers, Daniel Mohammadi, Camden Kurtz, Sarah Ingram and Jamie Parkerson for always being there to lighten the mood, help with experiments, and share food with. Lastly, I would like to thank my family: my wonderful supporting parents, Farhad and Suzanne Ghaffari, and my siblings Michael Ghaffari, Amanda Ghaffari and Carissa Ghaffari for their support, company and conversation throughout this two-year period.

TABLE OF CONTENTS

Page

LIST OF FIGURES

LIST OF ABBREVIATIONS

ActRIIA	Activin receptor, type IIA
ActRIIB	Activin receptor, type IIB
ALK2	Activin receptor-like kinase 2
ALK3	Activin receptor-like kinase 3
ALK6	Activin receptor-like kinase 6
ATP	Adenosine Triphosphate
BMP	Bone morphogenetic protein
BMPRIA	Bone morphogenetic protein receptor type IA
BMPRIB	Bone morphogenetic protein receptor type IB
BRII	BMP receptor type II
Ca^{2+}	Calcium ion
CaMK-II	Calcium/Calmodulin-dependent Protein Kinase Type II
$CaCl_2$	Calcium Chloride
CDMP	Cartilage-derived morphogenetic protein
CNCC	Cranial neural crest cells
Dhh	Desert hedgehog
Disp	Dispatched
EAD	Early anterior domain
ERK	Extracellular signal-regulated kinase
FGF	Fibroblast growth factor
GDF	Growth and differentiation factors
Gli	Glioma-associated oncogene family members
Hh	Hedgehog
Ihh	Indian hedgehog
JNK	C-jun-N-terminal kinase
KCl	Potassium chloride

MAPK	Mitogen-activated protein kinase
$MgSO_4$	Magnesium sulfate
MIP	Maximal intensity projection
NaCl	Sodium chloride
NSOFC	Nonsyndromic orofacial cleft
OP	Osteogenic proteins
PDGF	Platelet-derived growth factor
PFA	Paraformaldehyde
PI3K	Phosphoinositide 3-kinase
PKC	Protein kinase C
Scube2	Signal peptide CUB EGF-like domain-containing protein
Ser	Serine
Shh	Sonic hedgehog
Smo	Smoothened
TGFβ	Transforming growth factor β
Thr	Threonine
Wnt	Wingless-related integration site

Abstract

Establishing Zebrafish (Danio Rerio) as a Model for Orofacial Research

By Kevin Amir Ghaffari, B.S.

A thesis submitted in partial fulfillment of the requirements for the degree of Master of Science at Virginia Commonwealth University

Virginia Commonwealth University, April 2017

Major Advisor: Robert M. Tombes, Ph.D., Vice Provost, Department of Life Sciences

Across species, the face and more specifically the mouth, serves as an essential facet of everyday life. Amongst humans the mouth serves as a tool for the ingestion of food, a marker for facial recognition and a medium for communication. In order for the mouth to properly form, a series of precise growth and fusion events are needed. In order to insure that these events are orchestrated properly is a wide array of signals, transcription factors and epigenetic regulators. Due to the needed precision of these events, congenital birth defects of the face such as cleft lip and cleft palate are some of the most common worldwide.

In order to support existing and identify new developmental processes involved in mouth formation, we have utilized the effective model, *Danio* to study the molecules and events implicated in orofacial development. This was accomplished by developing a novel confocal imaging technique that allows for visualization of the forward facing zebrafish. Using this imaging technique we were able to establish when the embryonic

mouth first forms in zebrafish. Additionally, we recapitulated cleft-palate phenotypes shown in previous literature with the imaging method. Utilizing this technique, we then sought to further establish the role of Ca^{2+} signaling in proper orofacial morphogenesis and determine if the serine/threonine protein kinase, Ca^{2+}/calmodulin-dependent protein kinase type-II (CaMK-II), has a role in proper orofacial developmental.

Introduction

Embryonic (Primary) Mouth Formation

The embryonic or primary mouth is the term used to identify the initial opening between the foregut and the external environment (Dickinson and Sive, 2006). The primary mouth forms from a region that is missing mesoderm and is known as the Early Anterior Domain or EAD (Dickinson and Sive, 2006, 2007). The EAD serves as a signaling center that coordinates development of the face with its multifunctional role. Transforming the primary mouth into that of the secondary or adult mouth is a multistep process, starting with the removal of the basement membrane that separates ectoderm and endoderm in the EAD (Dickinson 2016). In vertebrates, neural crest quickly migrates anteriorly after the loss of the basement membrane and surrounds the primary mouth, guided by signaling that originates in the EAD (Dickinson and Sive, 2006; Soukup et al., 2013). In mammals and amphibians, the mouth opening is produced after contact is made between invaginating primary mouth ectoderm and foregut endothelium in a depressed region known as the stomodeum (Dickinson and Sive 2009; Soukup et al., 2013; Waterman, 1977, 1985). In *Xenopus*, stomodeal ectoderm and endodermal layers are reduced via apoptosis in what ultimately leads to perforation of the buccopharyngeal membrane (Dickinson and Sive, 2006). Different from this, the rupture of the buccopharyngeal membrane and formation of the zebrafish mouth opening is thought to occur after changes in intercellular junctions and cell orientations (Hamlett et al., 1996; Waterman and Kao, 1982). While the specific mechanisms controlling the rupturing of this oral membrane are unknown, there are a host of abnormalities implicated when it is not properly ruptured such as persistent buccopharyngeal

membrane and resulting choanal atresia (Verma 2009). Despite the clear importance of the embryonic mouth, there is a lack of data on what factors are necessary for this structure to form and how disruptions to the embryonic mouth's development could ultimately effect secondary mouth development.

Primary Palate, Midface and Upper Lip Formation

Arising from the embryonic mouth are several structures, namely the primary palate (and secondary palate for amniotes), midface and upper lip. By the fourth week of development the human face begins to form with migrating neural crest cells combining with mesoderm and the epithelial cover to establish the facial primordia (Jiang 2006). From here neural crest-derived facial mesenchyme contributes to the facial skeleton whereas mesoderm-derived cells form the muscles found in the face (Noden, 1978; 1983; 1988). The primary palate forms from the fusion of the maxillary, medial nasal and lateral nasal prominences in a series of highly regulated events. While the differences seen in head shape between organisms are more than likely initiated during embryonic development, there are negligible differences between species at early stages of facial development (Abzhanov et al. 2004). Something to note, however, is that some differences do exist between amniotic and non-amniotic models as it appears direct fusion events occur in fish species without the need for a midline epithelial seam (Swartz 2011). Furthermore, amniotes have a secondary palate that forms via outgrowths of the maxillary prominences, a structure that has been heavily implicated in cleft palate pathogenesis. Nevertheless, a host of recent genetic studies have shown the value zebrafish have as a model organism for palate research. As an

example, disruption of SHH causes defects in the palatal skeleton for human, mouse and zebrafish (Belloni et al., 1996; Chiang et al., 1996; Eberhart et al., 2006).

Signaling Pathways Implicated in Mouth Formation

Proper development of the orofacial region is controlled by species specific fusion events between the maxillary, medial nasal, and lateral nasal prominences. Differences between where these fusion events occur is what ultimately leads to the differences in head shape between organisms. Controlling these events in chick, mouse and zebrafish are major developmental signaling pathways such as BMP, HH, FGF, PDGF and Wnt (Dickinson 2016). While these developmental pathways have independent roles in orofacial morphogenesis, there has also been evidence of genetic cross-regulation as well as crosstalk intracellularly to control aspects of tissue patterning and cell proliferation (Jiang 2006). Previous literature showed inhibition of both BMP and HH signaling would lead to cleft-like phenotypes, something we wished to recapitulate with our new imaging technique.

BMP Signaling Pathway

The bone morphogenetic protein (BMP) family represents a class of signaling molecules that play a role in cell proliferation, morphogenesis, survival and differentiation during development. BMPs are multifunctional morphogens belonging to the TGFβ (transforming growth factor β) superfamily of signaling molecules. In the orofacial region, BMP signaling is crucial for the regulation of cell proliferation, extracellular matrix synthesis, and cellular differentiation (Mukhopadhyay 2008). BMPs were first identified and isolated from demineralized bone matrix and characterized due

to their function in ectopic bone formation in vivo (Wozney et al. 1988; Lyons et al. 1990). Afterwards, these same growth factors were found to be expressed widely in the vertebrate embryo and fetus where they were seen to have significant roles in regulation of neurogenesis, ossification, organogenesis and more (Lyons et al. 1990; Hogan, 1996a; Kishigami et al., 2004). BMP family members are known as one of three classes, either osteogenic proteins (OP), cartilage derived morphogenetic proteins (CDMP), or growth and differentiation factors (GDF). From these classes, BMPs are further derived into subfamilies based on sequence homology and phylogenetic analysis (Hogan, 1996b). BMP signaling is initiated by growth factor interaction between the type I (ALK2, ALK3, BMPRIA, ALK6, BMPRIB) and type II (BRII, ActRIIA, ActRIIB) receptors (von Bubnoff and Cho, 2001; Nohe et al., 2004). After activation by the appropriate BMP ligand, hetero-oligomers are formed by the type I and type II receptors, which then leads to initiating Smad-mediated intracellular signaling cascades that regulate transcription and expression of various target genes. BMP-induced receptor activation starts two different types of signaling pathways, the canonical pathway and the mitogen-activated protein kinase (MAPK) pathway. The canonical pathway involves activation of receptor-specific Smad 1, 5, and 8, followed by formation of a complex including the common Smad, Smad 4, which translocates into the nucleus to regulate transcription of BMP target genes (Yamamoto et al., 1997; Hollnagel et al., 1999; Nohe et al., 2004). The MAPK pathway includes p38, c-jun-N-terminal kinase (JNK), and extracellular signal-regulated kinase (ERK) pathways (Gallea et al., 2001; Zhao et al., 2002). Additionally, BMPs have been linked to activating PI3 kinase and PKC pathways (Kishigami and Mishina, 2005). After entering the nucleus, BMP type I receptor-specific Smads (BR-

Smads), Smad 1, 5, and 8, interact with DNA binding proteins which bind to specific sequences known as Smad-binding elements (SBEs) in the promoters of BMP target genes (Ogata et al., 1993; Korchynskyi et al., 2003). Targeting these genes in combination with BMP treatment and inhibition allows us to study the developmental significance of BMP signaling.

BMP Signaling Pathway in Craniofacial Development

Several studies show that BMP signaling plays a pivotal role in proper development of the orofacial region (Mukhopadhyay 2008). BMP has been implicated in the early patterning of the head, the development of cranial neural crest cells, apoptosis regulation and facial patterning. BMP signaling also helps regulate development of mineralized structures such as cranial bones, maxilla, mandible, palate and teeth. BMP has also been implicated to play a role in proper orofacial morphogenesis and cleft palate formation as it is suspected that its regulation of proliferation in the anterior palatal shelf mesenchyme and its ability to modulate apoptosis are the key factors as to whether the developing mouth is perturbed or not. Furthermore, it is possible that the small differences in BMP signaling are what ultimately lead to the variability in human craniofacial features as well as the differences seen in tissue physiology and disease susceptibility (Graf 2015). Literature also shows that CNCC must receive BMP signaling for proper palate development in zebrafish. BMP signaling has been implicated in mediating differentiation and/or survival/proliferation of palatal precursors after condensing upon the oral ectoderm (Swartz 2011). Both the anterior crest and the oral ectoderm have been shown to express bmp2b from 36 to 48hpf (Swartz 2011). Similarly, bmp4 was shown to be expressed in anterior CNCC and the oral ectoderm

from 36 to 40hpf (Swartz 2011). Beginning at 44 and 48hpf, a small population of posterior CNCC express bmp4, with the oral ectoderm weakly expressed bmp4 between 44 and 72hpf (Swartz 2011). Moreover, literature shows that BMP signaling is required for proper palatogenesis and craniofacial development in zebrafish. When using smad5 mutant fish in which downstream Bmp receptor signaling is defunct, the palatal skeleton is almost entirely lost with only small amounts of the trabeculae and surrounding cartilages remaining (Swartz 2011; Liu et al., 2005).

Hh Signaling Pathway

The Hedgehog signaling pathway plays a key role in normal vertebrate development (Lee et al., 2006; Briscoe and Therond, 2013) and maintenance of postnatal tissue homeostasis (Petrova and Joyner, 2014). Mammals have three Hedgehog-family members, Indian hedgehog (Ihh), Desert hedgehog (Dhh), and Sonic hedgehog (Shh); of these three, Shh has the most pivotal role in regulating developmental processes (Cobourne 2016). Shh is released from the surface of signaling cells as a dual-lipidated protein that can be modified by addition of cholesterol and palmitate groups at the C and N-terminal regions, respectively (Pepinsky et al., 1998; Porter et al., 1995). In order for Shh to be secreted from the cell a combined activity is needed between Dispatched (Disp), a multipass sterol-sensing domain protein (Caspary et al., 2002; Kawakami et al., 2002; Ma et al., 2002) and Scube2 (Signal peptide CUB EGF-like domain-containing protein), a secreted glycoprotein; both of these proteins interact with Shh through its cholesterol moiety (Creanga et al., 2012; Tukachisnky et al., 2012). Once secreted, Shh can go on to signal within embryonic tissues at long and short-range (Gritli-Linde et al., 2001). Reception at target cells is

mediated primarily through Patched1 (Ptch1), a twelve-pass transmembrane protein, which functions as a ligand-independent inhibitor in its resting state (Goodrich et al., 1996). If Shh is absent, Ptch1 accumulates and represses the activity of Smoothened (Smo), a G-protein coupled receptor (GPCR)-like protein (Corbit et al., 2005; Rohatgi et al., 2007) that is essential for signal transduction (Zhang et al., 2001). Downstream of interactions between Smo and Ptch1, intracellular signaling is coordinated directly via processing of Gli (Glioma-associated oncogene family members; Gli 1-3) transcription factors and gating their entry into the nucleus (Haycraft et al., 2005). Modulating the interaction between Shh, its receptors, and the direct transcriptional targets it has (Gli1, Ptch1, Hhip1) allows for us to explore the role Hh signaling has on development of the zebrafish face.

Hh Signaling Pathway in Craniofacial Development

Hedgehog signaling has been implicated in driving outgrowth of the upper face (Hu et al. 2003; Hu & Marcucio, 2009) as well as patterning the midline for both the brain and the face (Chiang et al. 1996). Proper temporal based expression of Shh, the most studied ligand in the hedgehog signaling pathway, is critical for proper development of the embryonic facial ectoderm, neuroectoderm, pharyngeal endoderm and the outgrowth of the frontonasal process (Cordero et al., 2004). Lack of proper Shh expression has been implicated in facial clefting while overexpression has been linked to widening of the head leading to a condition known as hypertelorism. Interestingly, early hedgehog signaling was also shown to regulate primary mouth size in *Xenopus* as well as having a role on oral opening size throughout development (Liu 2014). Furthermore, crosstalk between Shh and the BMP signaling pathway has been well

documented and Shh signaling has been shown to play a pivotal role in coordinating reciprocal epithelial-mesenchymal interactions between FGFs, BMPs, cyclins and Fox transcription factors that appear to be essential for normal palatal development (Hu 1999). It has also been shown that, as in mouse, the oral ectoderm of zebrafish also expresses Shh (Miller et al., 2000). In fact, after a more detailed study of expression patterns by Swartz et al., it was shown that the oral ectoderm strongly expresses Shh throughout palatogenesis in zebrafish (Swartz 2011). Lastly, in zebrafish, separate early and late requirements for Hh signaling have been shown. When fish were treated with higher concentrations (50-100μM) of the Smoothened antagonist cyclopamine for any 4-hour period between 0 and 24hpf it caused a complete loss of the anterior neurocranium, showing an absolute requirement for Hh signaling in anterior neurocranium development during NC migration (Wada 2005). Oddly enough, 50μM cyclopamine treatments of embryos older than 24hpf (after NC migration has taken place) still disrupted trabecular and ethmoid development (Wada 2005). Treatment between 30-35hpf eliminated the medial ethmoid plate while trabecular cartilages were still well formed, resulting in a large palatal cleft (Wada 2005). Only after 48hpf were treatments seen to be non-effective at causing abnormalities in palatal development.

Ca^{2+} Signaling in Craniofacial Development

In order to explore new territory with our imaging technique we decided to investigate the role of Ca^{2+} signaling in orofacial morphogenesis. Ca^{2+} supplementation has been linked with a reduced risk of developing NSOFC (Nonsyndromic orofacial cleft) (Sabbagh et al. 2015) and lower blood calcium levels are linked to the often cleft-associated DiGeorge syndrome. CaMK-II has been implicated in tongue abnormalities

in mice which typically led to facial morphological defects such as cleft palate (Xiao et al. 2014). Furthermore, our lab has previously shown CaMK-II to have a role in cloacal cilia stabilization, opening up the possibility for CaMK-II to have a role stabilizing cilia elsewhere, such as the face. Making a connection between Ca^{2+} signaling and zebrafish palatogenesis is a way to show the strength of our technique when investigating pathways that are not as explored.

CaMK-II

Ca^{2+}/Calmodulin-dependent protein kinase type II (CaMK-II) is a ubiquitously expressed serine/threonine protein kinase. CaMK-II is encoded by four genes (α, β, γ, δ) in mammals, producing over thirty-five different splice variants (Tobimatsu et al., 1989; Schworer et al., 1993; Hudmon and Schulman, 2002; Tombes et al., 2003). The CaMK-II holoenzyme contains 12 functional subunits. Each subunit has an amino terminal catalytic domain that is followed by an autoregulatory domain, a series of variable inserts, and a carboxyl terminal association domain. The catalytic domain contains an ATP binding site that has a specific sequence for substrate binding which leads to subsequent phosphorylation and activation. The mediator of the holoenzyme's activity is the autoregulatory domain. Within this sequence of residues is an autoinhibitory domain, an autophosphorylation site, and a CaM (calmodulin)-binding site. When CaM binds to its domain (residues 296-311), the catalytic domain is no longer inhibited and is free to phosphorylate protein substrates, including itself, at $Thr^{286}(\alpha)/Thr^{287}(\beta, \delta, \gamma)$ which is key to its role in many signal transduction pathways (Braun and Schulman, 1995). The various isoforms of CaMK-II differ in their tissue expression, cellular localization, and sub-cellular compartmentalization (Schworer et al., 1993; Brocke et al., 1995; Bayer

et al., 1999; Tombes et al., 1999; Soderling et al., 2001; Hudmon and Schulman, 2002). In response to increased levels of intracellular calcium, CaMK-II phosphorylates a diverse set of substrates of the cytoskeleton, sarcoplasmic reticulum, and the post-synaptic density (Braun and Schulman, 1995). Once activated, these protein substrates form complexes of scaffolding molecules for signal transduction and other neuronal pathways. The extensively studied alpha CaMK-II has been implicated in behavior, memory, long-term potentiation and neuronal plasticity. In zebrafish, CaMK-II is encoded by seven genes (α, β1, β2, γ1, γ2, δ1, δ2). Over 20 splice variants have been identified from these seven genes, with the variants existing in locations that indicate CaMK-II has a multi-functional role in transducing Ca^{2+} signals in the earliest phases of vertebrate development (Rothschild et al., 2007). Amongst these regulatory roles, zebrafish CaMK-II has been implicated in central nervous system function, convergent extension movements, axis formation during gastrulation, inner ear development, and more (Rothschild et al., 2013; Rothschild et al., 2007).

Zebrafish as a Model for Orofacial Morphogenesis

While the human face does not resemble the zebrafish (Danio Rerio) face, both humans and zebrafish are deuterostome vertebrates with conserved developmental pathways and mechanisms. For example, it has been documented that portions of the first stream of CNCC in zebrafish come to occupy frontonasal and maxillary domains as can be seen with its amniotic model counterparts. By 60hpf these cells have given rise to specific subsets of the palate with a more critical time period of dynamic cell rearrangements occurring between 36 and 48hpf, ultimately driving the morphogenesis of the zebrafish palate (Swartz 2011). Due to zebrafish developing faster than other

organisms currently used for orofacial research (chick, frog, mouse) *Danio* is a promising model for discovery of new molecules required for orofacial development at specific time periods. Furthermore, zebrafish serve as an excellent model organism due to their rapid high-yield of offspring and ease in which genetic changes may be introduced. Another important feature to note is that zebrafish embryos are completely transparent which allows for non-invasive imaging techniques when manipulating genes and monitoring development. Despite the strength of *Danio* as a model organism for embryonic development the majority of attention has been placed on adult jaw, teeth, and skull formation in zebrafish due to the large degree of cartilage and bone growth and ease in which Alcian blue and Alizarin red staining can be utilized. Moreover, our lab believes researchers have previously avoided using zebrafish to study early mouth development due to the misconception that *Danio's* developing body curvature would prevent imaging the face clearly. Navigating around the fears of early zebrafish face imaging, we were able to capitalize on the rapid development of *Danio* and show the strength this organism has in not only recapitulating phenotypes seen in mammalian models but also for exploring new areas of orofacial research.

Materials and Methods

Zebrafish strains and care

Wild type (AB and WIK), Tg(*Fli1:GFP*), and Tg(Hsp70I:CA Alk6-p2a-Kikume) fish embryos were obtained through natural matings and raised at 28.5°C, as described previously (Kimmel et al., 1995). *Fli1:GFP* transgenic embryos express GFP in cartilage-producing cells as well as vasculature (Lawson and Weinstein, 2002).

CaMK-II inhibition

Zebrafish embryos were incubated in 10 μM KN-93 in 2 ml of E3 (5.0mM NaCl, 0.17mM KCl, 0.33mM $CaCl_2$, 0.33mM $MgSO_4$) continuously, starting at 24, 48, and 50hpf respectively. At 72hpf the embryos were pipetted out of solution and treated and fixed in 4% paraformaldehyde. After 24 hours they were pipetted into individually labeled Eppendorf tubes and washed 3-4x with PBTx. Next the embryos were counter stained with Rhodamine Phalloidin (1:500) and left in a refrigerator wrapped in aluminum foil for 24 hours. After 24 hours, the embryos were washed 3-4 more times with PBTx and then prepared for imaging. Embryos were not typically dechorionated prior to treatment.

BMP inhibition

Zebrafish embryos were incubated at 28.5°C in 10 μM DMH1 in 2 ml of E3 continuously, starting at 24, 42, and 48hpf respectively. At 72hpf the embryos were pipetted out of solution and fixed with 4% paraformaldehyde. After 24 hours they were pipetted into individually labeled Eppendorf tubes and washed 3-4x with PBTx. Next the embryos were counter stained with 1μL Rhodamine Phalloidin and left in a refrigerator

wrapped in aluminum foil for 24 hours. After 24 hours, the embryos were washed 3-4 more times with PBTx and then prepared for imaging. Embryos were not typically dechorionated prior to treatment.

Hedgehog inhibition

Zebrafish embryos were incubated in 100 µM cyclopamine in 2 ml of E3 continuously, starting at 22 and 44hpf respectively. At 72hpf the embryos were pipetted out of solution and treated with PFA 4%. After 24 hours they were pipetted into individually labeled Eppendorf tubes and washed 3-4x with PBTx. Next the embryos were counter stained with 1µL Rhodamine Phalloidin and left in a refrigerator wrapped in aluminum foil for 24 hours. After 24 hours, the embryos were washed 3-4 more times with PBTx and then prepared for imaging. Embryos were not typically dechorionated prior to treatment.

CaMK-II antibodies

Immunolocalization using anti-autophosphorylated CaMK-II (anti-P-CaMK-II; phosphorylated at Thr^{287}), CaMK-II and total CaMK-II antibodies has previously been described by this laboratory (Easley et al., 2006; Rothschild et al., 2011). The anti-phospho-Thr^{287} (anti-P-T^{287}) antibody detects CaMK-II proteins across species and the total CaMK-II antibody reacts with the C-terminal region of all CaMK-II proteins.

Alk6 heat shock

A previously generated heat-shock inducible constitutively active BMP receptor 1B plasmid was used as previously described (Row et al., 2016). In short, the coding sequence of a mutant constitutively active (Q207D) mouse *ALK6* (*caalk6*) without the

stop codon was inserted into a heat-shock vector to create *hsp70l:caalk6-p2a-NLS-kikume* (abbreviated *HS:caalk6*) flanked by *tol2* transposable element arms (Macias-Silva et al., 1998). A stable transgenic line of *HS:caalk6* was generated by injecting the plasmid DNA along with in vitro transcribed *tol2* transposase mRNA (25 pg of each per embryo) into 1-cell stage embryos and screening injected animals when they became adults for germ-line transmission (Kawakami, 1998). Embryos were incubated at 40°C for thirty minutes in a water bath to activate the CA ALK6 ubiquitously. We would like to thank the Martin lab for providing us with this line.

Confocal Microscopy

Two different confocal microscopes were used for imaging the forward facing zebrafish embryos. In order to image the faces, a novel technique was developed (Figure 5). First, fish were raised to desired developmental time point (typically 72hpf) and fixed with PFA 4% in respective Eppendorf tubes. After 24 hours, PFA was washed out with PBTx 3-4 times and 1µL of Rhodamine Phalloidin was added to solution. After 24 hours 3-4 more PBTx washes were performed. At this time the fish were pipetted from the Eppendorf tubes and into a small petri dish with 100% glycerol. Once in the petri dish, a small cutting utensil was used to precisely cut off the faces which were then pipetted onto a mounting slide. Using 3-4 cover slips per side on the mounting slide, the slide was mounted onto a confocal microscope and focused appropriately. Slight adjustments were made using fingers until the face was forward facing. Once forward facing, the image was focused on up to 20x magnification and was converted into a MIP (Maximal intensity projection) so that all sections of the z-stack are represented. Due to

confocal imaging of the face throughout the entire z-plane of the skull, we can visualize the internal features of the mouth in addition to the external protruding mouth.

Face Measurements

In order to quantify the qualitative fish face images that have been generated from our experiments a series of measurements were taken and compared between experimental and control groups. Eight measurements were utilized for each fish face: a brain measurement (height from top of skull to above upper mouth region), distance between outside of the eyes (width of head), distance between inner eyes (intercanthal distance), width of the top and bottom of the mouth at both the protruding level of the z-stack as well as the internal portion of the z-stack, and mouth height from top to bottom. These measurements were then averaged and graphed, with error bars on each categorical measurement representing the standard deviation within each group. With these facial measurements statistical analyses were performed using the program JMP Pro 12. T tests were utilized comparing control and treatment group fish face measurements and whether a significant difference existed in measurements between the groups.

Fish Face

We believe our work will make significant contributions to FishFace, a publicly accessible atlas for zebrafish craniofacial development. Currently FishFace focuses on pharyngeal arch formation and skull anatomy and has no data on mouth formation in the zebrafish. By focusing on these later stages of development and analyzing when ossification of the zebrafish skull occurs there has been a neglect in the area of

research where the zebrafish shines as a model organism, the early embryonic stages. By elucidating mouth formation, developmental timing and the embryonic development patterns associated with proper mouth formation we can give the zebrafish craniofacial community new information to study primary palate abnormalities such as cleft lip and cleft palate.

Results

Identifying when the Zebrafish Mouth Opens

After reviewing literature on primary mouth formation by Dickinson et al. we decided to investigate when the primary mouth first forms in zebrafish and whether primary mouth formation can be studied in zebrafish (Dickinson 2016). First, a technique was developed to image the forward facing zebrafish so that its mouth, brain, and intercanthal distance could be easily measurable and visible (Figure 1, Figure 5). Additionally, the technique includes creating a MIP, or maximal intensity projection, which allows for analysis of the mouth not only externally but throughout the entire face and skull. Forward facing images are standard for most other model organisms when conducting craniofacial research. Utilizing the proposed technique, a series of developmental time points were tested in order to measure the technique's efficacy and determine broadly when the mouth is open in zebrafish. In order to do this, wildtype zebrafish were raised to 36, 48, 60, 72hpf, and 5dpf respectively. After fixing the embryos at the appropriate developmental time point, they were treated with Phalloidin 488 – allowing for us to image them using the new confocal microscopy technique (Figure 5). An external mouth was not visible at 36hpf but was visible at 48hpf. From this initial time point analysis, it was determined that the mouth first opens in zebrafish between 36hpf and 48hpf (Figure 2). After establishing that the mouth opens between 36hpf and 48hpf, we decided to investigate in more detail the exact time in which one can expect the zebrafish mouth to be open. Fixing embryos one hour apart between 36hpf and 48hpf resulted in our discovery that the zebrafish embryonic mouth is first open at approximately 45-46hpf (Figure 3, Figure 4). Furthermore, by imaging fish faces

during this range of early embryonic development we were able to confirm that the technique is viable despite natural body curvature in developing zebrafish (Figure 3). Moving forward, this knowledge of when the zebrafish mouth opening is formed was utilized to time future drug treatments in addition to being used as a reference point when considering normal orofacial morphogenesis and how morphogenesis may become impaired after being acted upon by various factors.

Recapitulating BMP Craniofacial Defects

Utilizing our new imaging technique, we decided to next be able to recapitulate the phenotypes previously seen in frog, fish, and mice when the BMP signaling pathway was antagonized (Swartz 2011; Liu et al., 2005; Mukhopadhyay 2008). Previously, inhibition of BMP signaling was shown to cause almost complete loss of the palatal skeleton (Swartz 2011; Liu et al., 2005) as well as loss of several cartilaginous structures (Schilling et al., 2011). In order to possibly recapitulate these abnormal phenotypes, the small molecule inhibitor DMH1 was used. DMH1 specifically antagonizes the intracellular kinase domain of BMP type I receptors, allowing for inhibition of basal Smad phosphorylation. We decided to treat developing Tg(*Fli1:GFP)* embryos with DMH1 at 24, 40, 42, and 48hpf respectively (Figure 6). After allowing for all of the embryos to develop to 72hpf, they were counterstained with Rhodamine Phalloidin. After mounting the fish and properly orienting their face forward, maximal intensity projections were created via confocal microscopy in order to compare the phenotypic effects of the antagonist when starting treatment at different developmental time points. Out of the four time points treated with DMH1, the 24hpf treatment group had the most prominent orofacial abnormalities (Figure 7). In order to quantify these

differences a series of measurements were created across consistent landmarks of the zebrafish face. Amongst the facial features that were observed via the MIPs are the brain length (top to bottom), the distance between the outside of the eyes (head width), the distance between the inside of the eyes (intercanthal distance), and the mouth height (top to bottom). Within the single z-stack images we also measured for the width of the top and bottom mouth both internally and externally (protruding mouth). From these measurements we were able to determine that not only did the fish faces have consistent orofacial clefting at this time point, they also had a smaller distance between their eyes and the width of the top and bottom of their outward mouth (Figure 8). This was interesting as it was the first indication that our imaging technique could also be used to observe defects in the skull that could then possibly modify mouth size and shape. After confirming our ability to recapitulate orofacial clefting with the use of DMH1, we decided to perform a heat shock experiment with a constitutively active HS:CA Alk6 transgenic line of zebrafish. By heat shocking for 30 minutes at 40°C at 18hpf we were able to induce overexpression of BMP signaling and look at the developmental outcomes when fixed at 72hpf. After counter-staining with Rhodamine Phalloidin a series of maximal intensity projections were created of both heat shocked fish and their control counterparts. Severe phenotypes were exhibited when heat shocked at 18hpf (Figure 9) showing a consistent cleft-like phenotype and distinct abnormalities in craniofacial shape and size. When comparing measurements of our established facial markers, there was a significant size difference seen between the heat shock fish and control fish for total mouth height ($p = 0.0415$), and the upper mouth internally ($p = 0.0455$) and externally ($p = 0.0275$) (Figure 10).

Recapitulating Hh Craniofacial Defects

Next, we sought to recapitulate the craniofacial defects exhibited by inhibition of another known key craniofacial development pathway, the Hedgehog signaling pathway (Hu et al., 2003; Cordero et al., 2004). Previous literature showed that inhibition of the Hedgehog signaling pathway can lead to loss of cartilage structures and impairment of neurocranium development (Wada 2005). In order to possibly recapitulate these phenotypes, we utilized the Smoothened antagonist cyclopamine and treated at two different time points, 22 and 44hpf. After allowing for all of the embryos to develop to 72hpf they were counterstained with Rhodamine Phalloidin. After mounting the fish and properly orienting their face forward, maximal intensity projections were created via confocal microscopy in order to compare the phenotypic effects of the antagonist when starting treatment at different developmental time points. Both the 22hpf treatment group as well as the 44hpf treatment group displayed clear cleft-like phenotypes as well as signs of other craniofacial abnormalities (Figure 11). When creating measurements of the fish faces using the same landmark features, we were able to determine that a difference existed between the control fish face and that of the 44hpf treatment group in regards to head width, intercanthal distance and the width of the upper protruding mouth (Figure 12). While significance levels could not be calculated for the 22hpf treatment group a significant size difference ($p = .0043$ and $p = .0476$ respectively) was seen between control lower protruding mouth size and upper internal mouth size when compared to fish incubated with cyclopamine at 44hpf (Figure 12). The distinct phenotypes we were able to generate with the cyclopamine treatments further

established the use of our imaging technique as a way to visualize disease states when studying the face.

CaMK-II's role in Craniofacial Development

In order to determine the role CaMK-II has in craniofacial development we decided to first look at expression levels of auto-phosphorylated and total CaMK-II in the mouth region. Using anti-autophosphorylated CaMK-II and total CaMK-II antibodies we were able to detect expression of both auto-phosphorylated CaMK-II surrounding the perforated mouth as well as total CaMK-II in the same region (Figure 13). After confirming that both P-CaMK-II and CaMK-II are expressed in the orofacial region we then decided to observe the effects of the calmodulin binding antagonist of CaMK-II, KN93. We decided to incubate zebrafish embryos with KN93 at three different time points: 24, 48, and 50hpf respectively. After allowing for all of the embryos to develop to 72hpf, they were counterstained with Rhodamine Phalloidin. After mounting the fish and properly orienting their face forward, maximal intensity projections were created via confocal microscopy in order to compare the phenotypic effects of the antagonist when starting treatment at different developmental time points. From these drug treatments the most severe craniofacial defects were exhibited by zebrafish treated at 48hpf (Figure 14). While the other treatment periods did show some qualitative signs of craniofacial abnormalities, it was not cleft-like and instead typically consisted of changes in the head shape/size, creating a box-like mouth (Figure 15). Changes in features surrounding the face that result in mouth morphological changes is what we anticipated as previous research showed a role for CaMK-II in regulating tongue formation that, when impaired, led to orofacial defects (Xiao et al. 2014). By measuring landmark facial

features we were able to establish some differences between the face size and shape in the drug treated fish and control fish. Namely, the 24hpf treatment group exhibited a somewhat larger brain and a smaller mouth from top to bottom (Figure 16). Comparing the 48hpf treatment group with the control showed a significant difference ($p = 0.0068$) in brain size, with minor changes to mouth width also occurring (Figure 16). Potentially causing the differences in mouth width and shape are the changes in brain size, causing the facial prominences to compensate and fuse at abnormal locations. In conclusion, antagonizing CaMK-II caused craniofacial defects, with the most common phenotype being that of a “boxed” mouth. Furthermore, changes in brain size were seen in multiple treatment groups, shedding light on another potential regulatory role for CaMK-II.

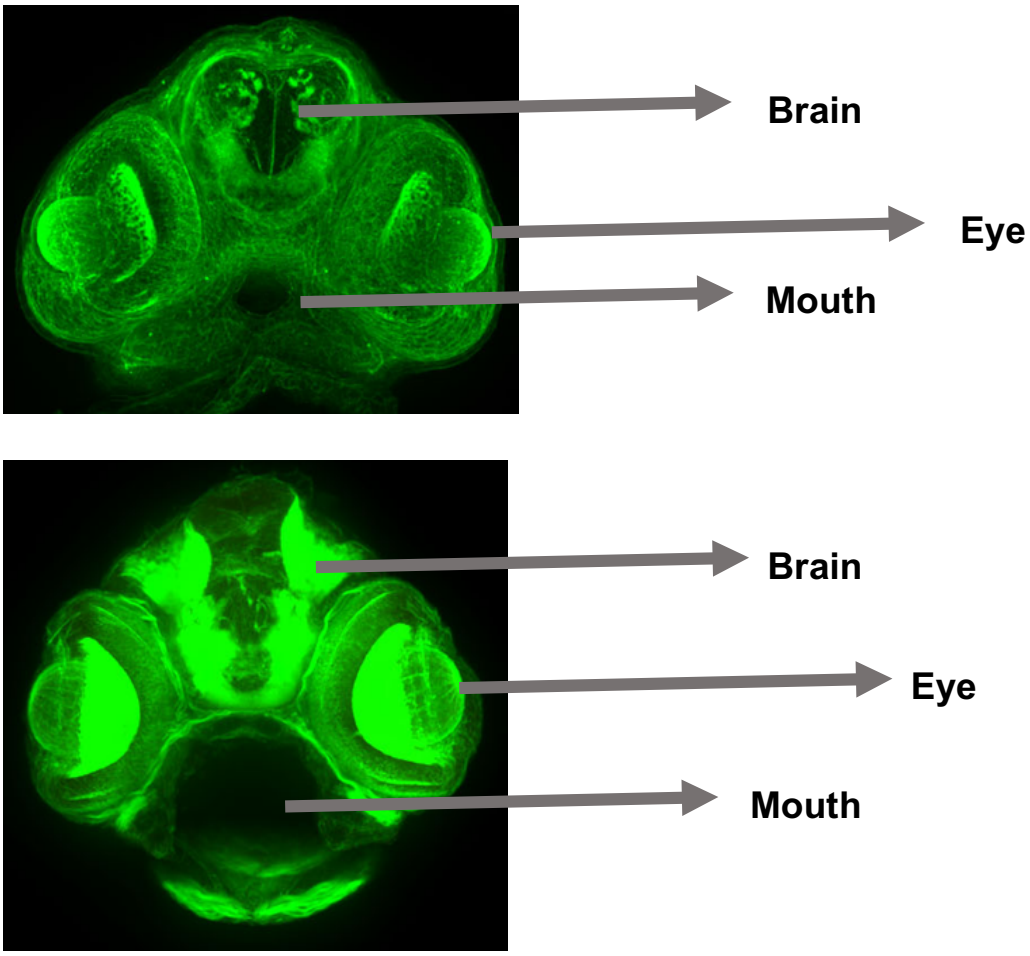

Figure 1. Zebrafish (Danio Rerio) Head Anatomy. Top – 48hpf, bottom – 5dpf. Wildtype fish treated with Phalloidin 488 after being fixed in 4% PFA at desired developmental time point. Both facial images are maximal intensity projections (MIPs) that include all sections of z-stack using confocal microscopy.

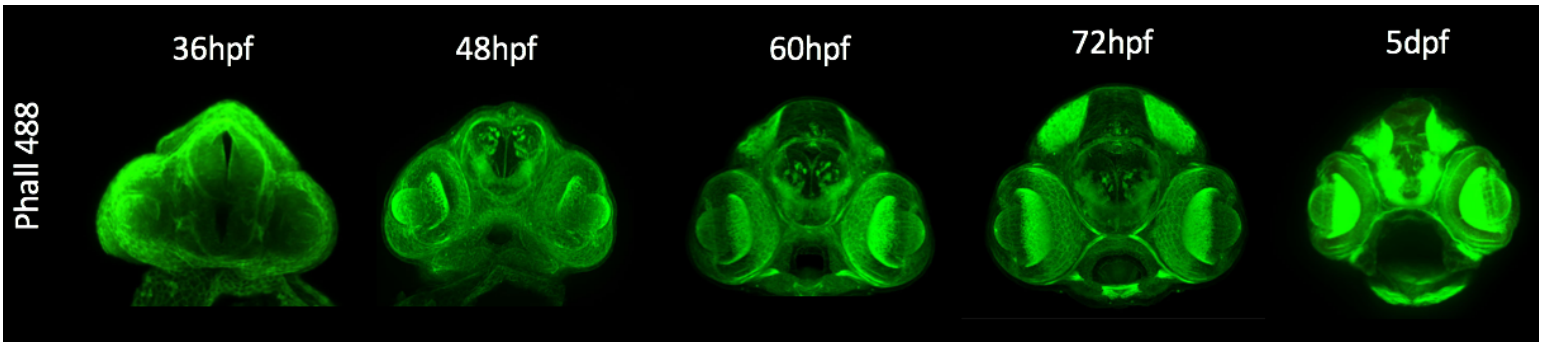

Figure 2. Development of Zebrafish (Danio Rerio) face at 36, 48, 60, 72hpf, and 5dpf. Wildtype fish stained with Phalloidin 488 after being fixed in 4% PFA at desired developmental time point. All facial images are maximal intensity projections (MIPs) that include all sections of z-stack using confocal microscopy.

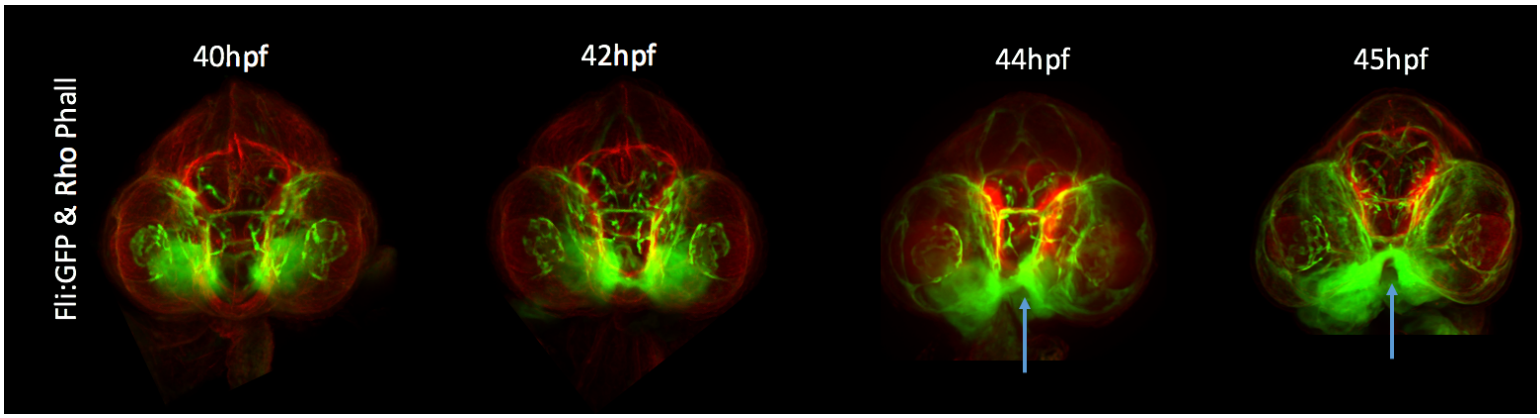

Figure 3. Development of Zebrafish (Danio Rerio) face at 40, 42, 44, and 45hpf. Tg(*Fli1:GFP)* fish counter-stained with Rhodamine Phalloidin after being fixed in 4% PFA at desired developmental time point. All facial images are maximal intensity projections (MIPs) that include all sections of z-stack using confocal microscopy.

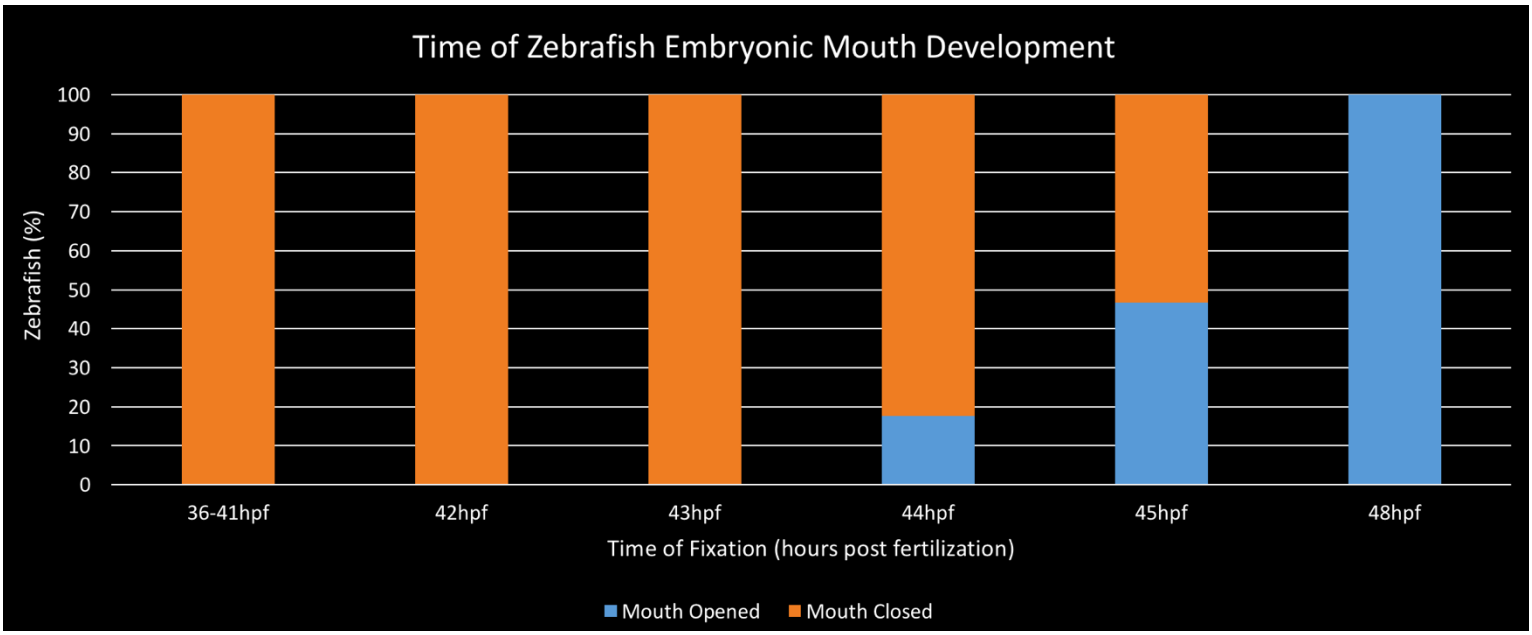

Figure 4. Development of Zebrafish (Danio Rerio) face at 36-41, 42, 43, 44, 45, and 48 hours post fertilization. When fixing fish before 44hpf no open mouth was observed. At 45hpf nearly 50% of the embryos had a visible mouth, indicating this is around the time of external perforation and opening of the embryonic mouth. Inherently the time point cannot be exact as there are small discrepancies such as when the eggs were harvested, developmental rate, etc. Therefore, we have determined the primary mouth opens at *approximately* 45-46hpf.

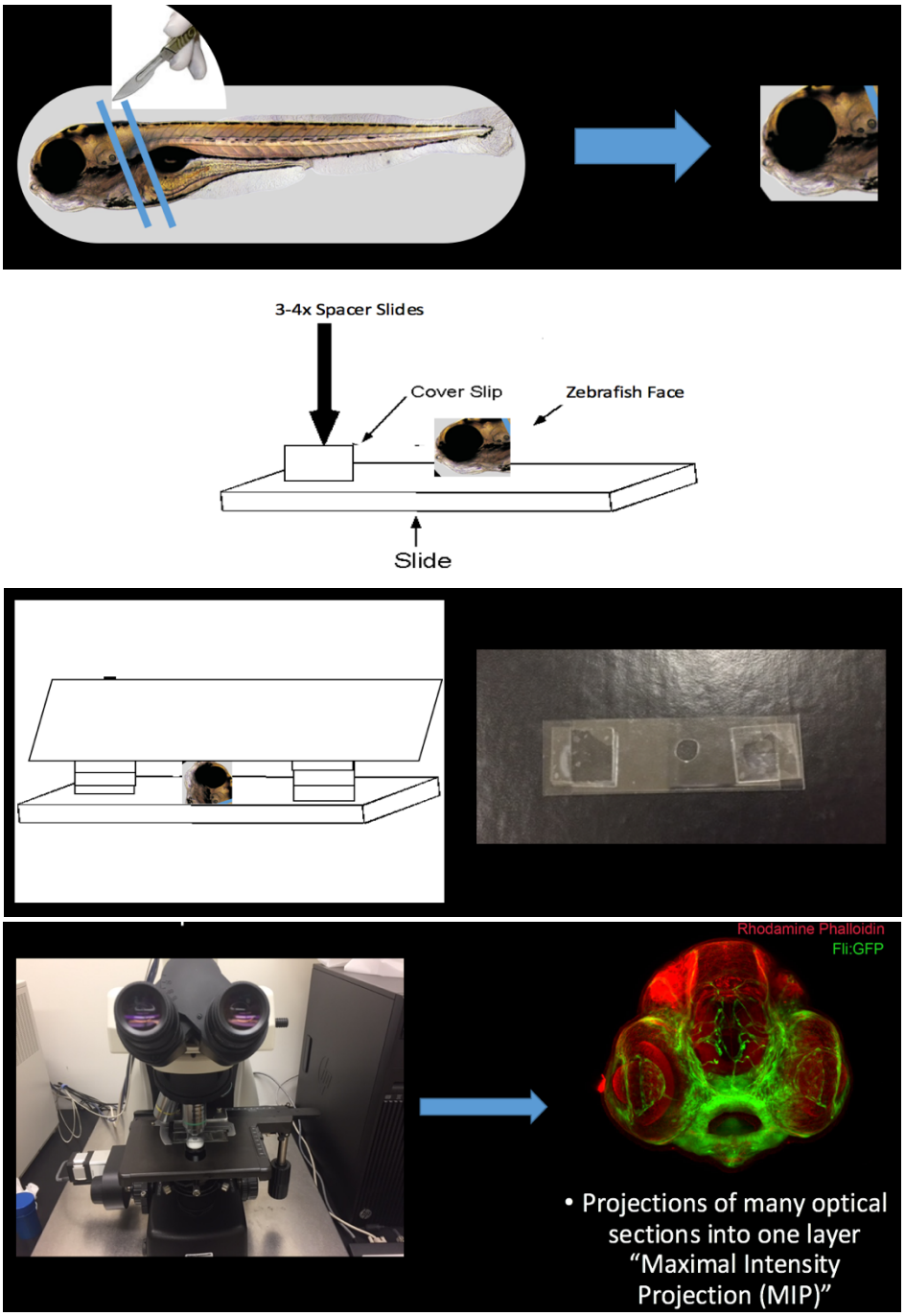

Figure 5. Technique used to mount and image forward facing zebrafish face. First, a fish that has been treated with PFA 4% and a stain (or counter-stain in the case of Tg(*Fli1:GFP*) fish) is pipetted into a dish with 100% glycerol and its face is separated from the body with a cut spanning behind the brain and lower jaw. After properly mounting the sectioned face onto a cover slide, adjustments are made to orient the face forward. Using the forward facing fish a MIP (Maximal Intensity Projection) is created using confocal microscopy in the NIS Elements software.

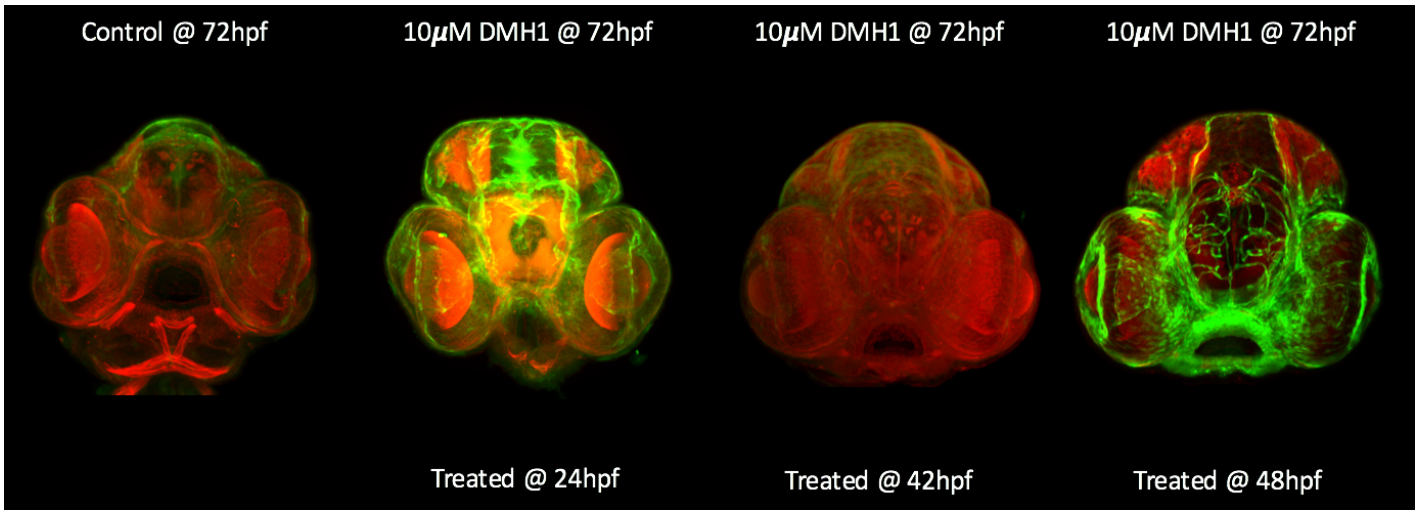

Figure 6. Drug treatments with BMP type I receptor antagonist, DMH1. Treatments were at 24, 42, and 48hpf, respectively. Once treated with DMH1, the fish were incubated at 28.5°C until 72hpf when they were fixed with 4% PFA and prepared for imaging. All fish were Tg(*Fli1:GFP)* fish counter-stained with Rhodamine Phalloidin after being fixed in 4% PFA. All facial images are maximal intensity projections (MIPs) that include all sections of z-stack using confocal microscopy. The most severe phenotypes were seen at the 24hpf treatment time period, exhibiting signs of orofacial clefting as well as a "box-shaped" mouth.

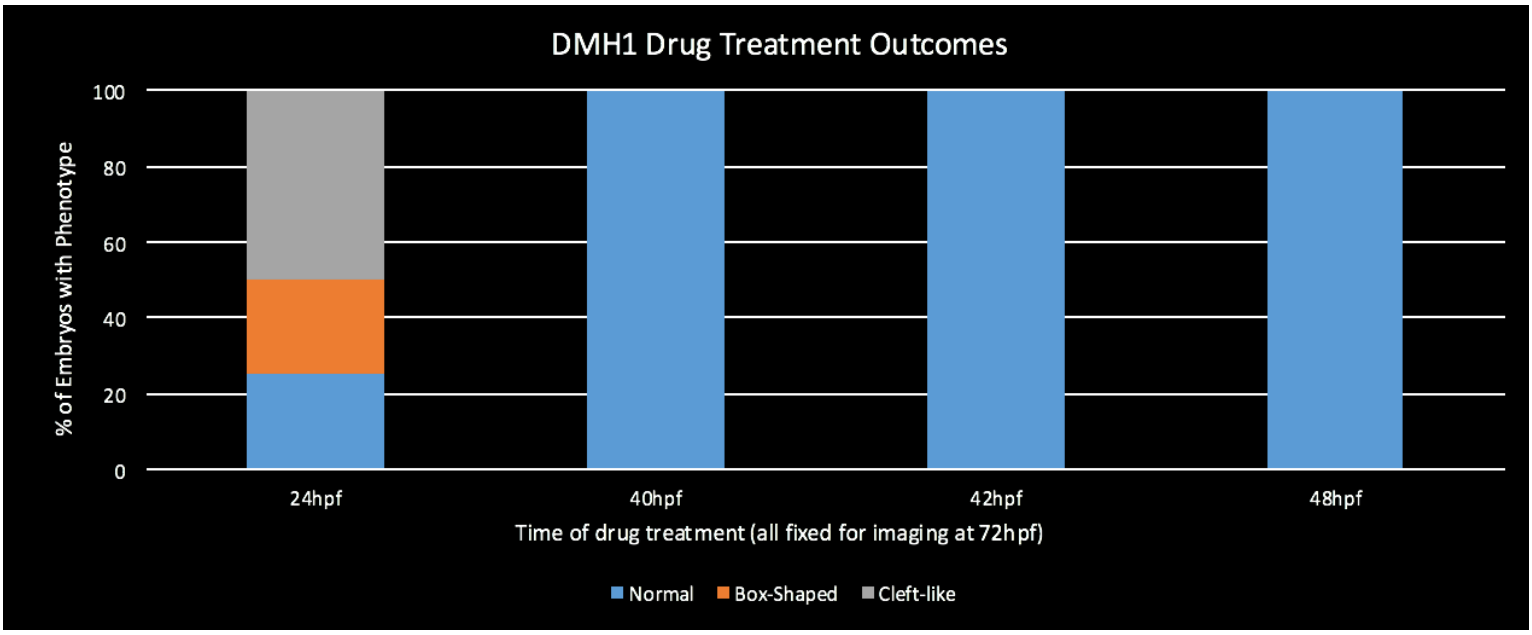

Figure 7. Drug treatment outcomes with BMP type I receptor antagonist, DMH1. Treatments were at 24, 40, 42, and 48hpf, respectively. Once treated with DMH1, the fish were incubated at 28.5°C until 72hpf when they were treated with 4% PFA and prepared for imaging. Bars represent the percentage of fish with phenotypic changes to mouth morphology, indicated as being phenotypically normal (blue), box-shaped (orange) or cleft-like (grey). From the results it was concluded that DMH1 treatment caused the most significant changes to facial development when treated at an earlier time point (24hpf). Treatment at later time points (40, 42, and 48hpf) did not show any discernible changes qualitatively, however subtle changes were seen in measurement analysis.

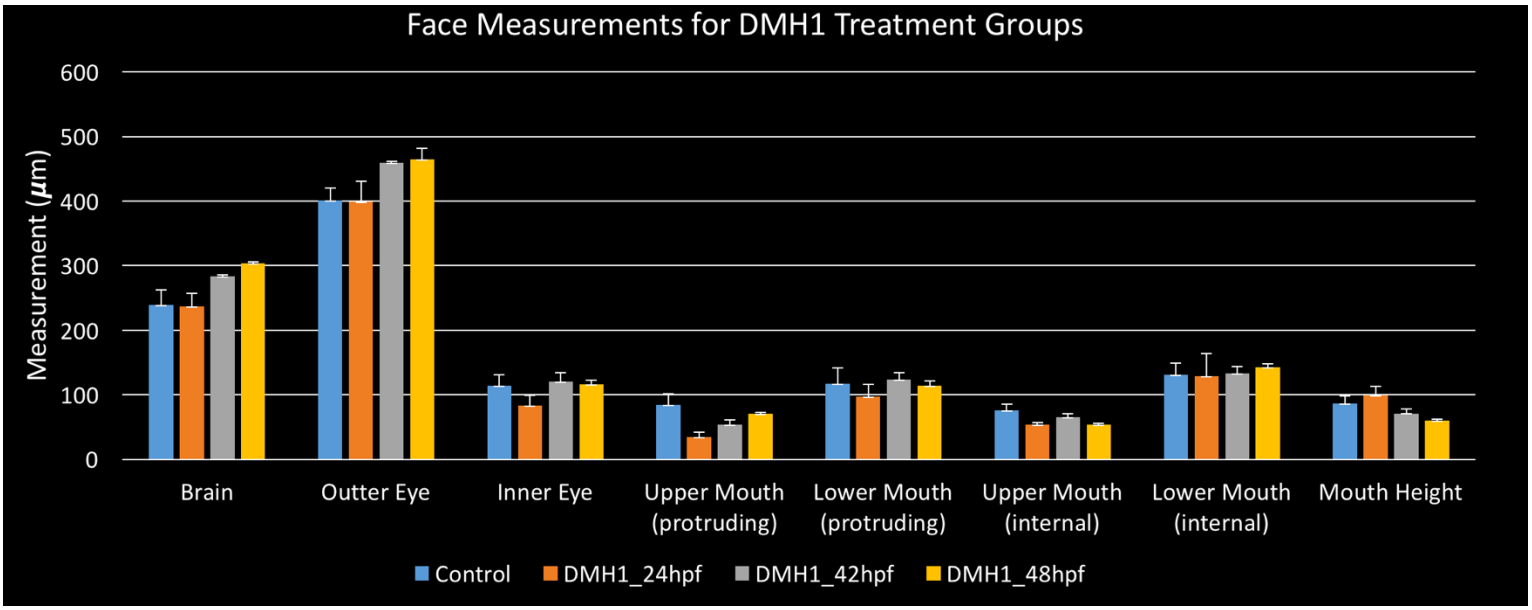

Figure 8. Measurement outcomes after treatment with BMP antagonist DMH1. Measurements of the face were performed with control, 24, 42 and 48hpf treatment group fish. Average measurements were compiled with a minimum n-value of 5 and compared across control and treatment fish. Each bar represents the average measurement value for given treatment group and measurement category. Error bars represent the standard deviation within the given treatment group or control. From this data it was determined that there was a difference between 24hpf treatment fish and control in terms of mouth size for the upper protruding mouth, lower protruding mouth and upper internal mouth. Other subtle changes were noted in the 42 and 48hpf treatment groups, such as the head width (outer eye measurement) in both groups.

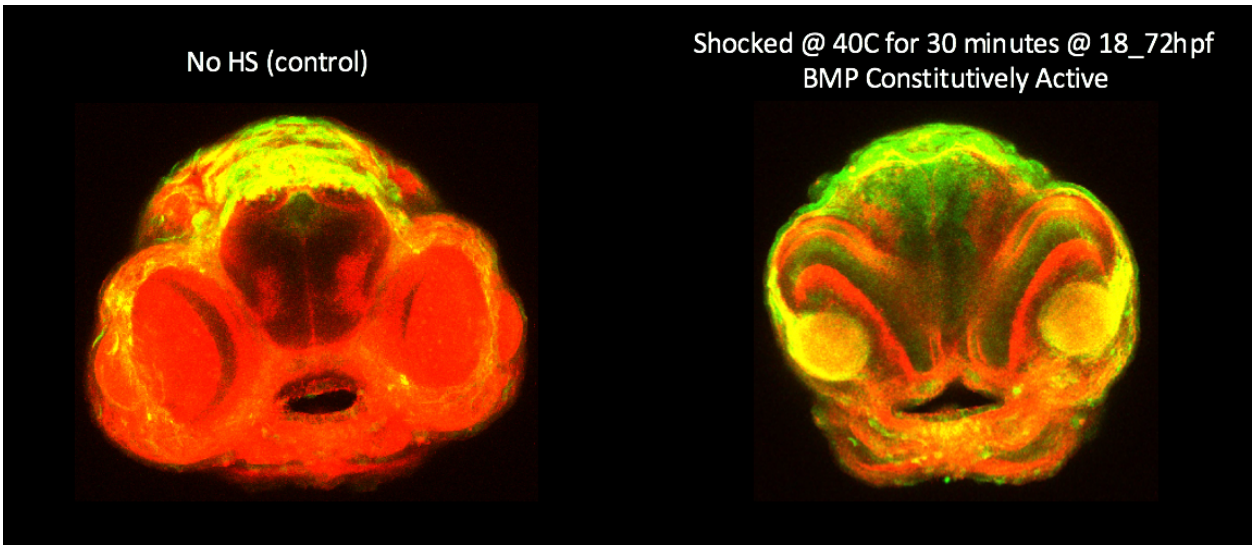

Figure 9. Heat shock experiment with constitutively active BMPR. A Hsp70I:CA Alk6 transgenic line was used to test constitutively active BMP signaling. Fish were shocked at 40°C for 30 minutes at 18hpf and then left to incubate until 72hpf when they were treated with 4% PFA and prepared for imaging. Severe phenotypes were exhibited, showing signs of orofacial clefting and disfigured head shape and size.

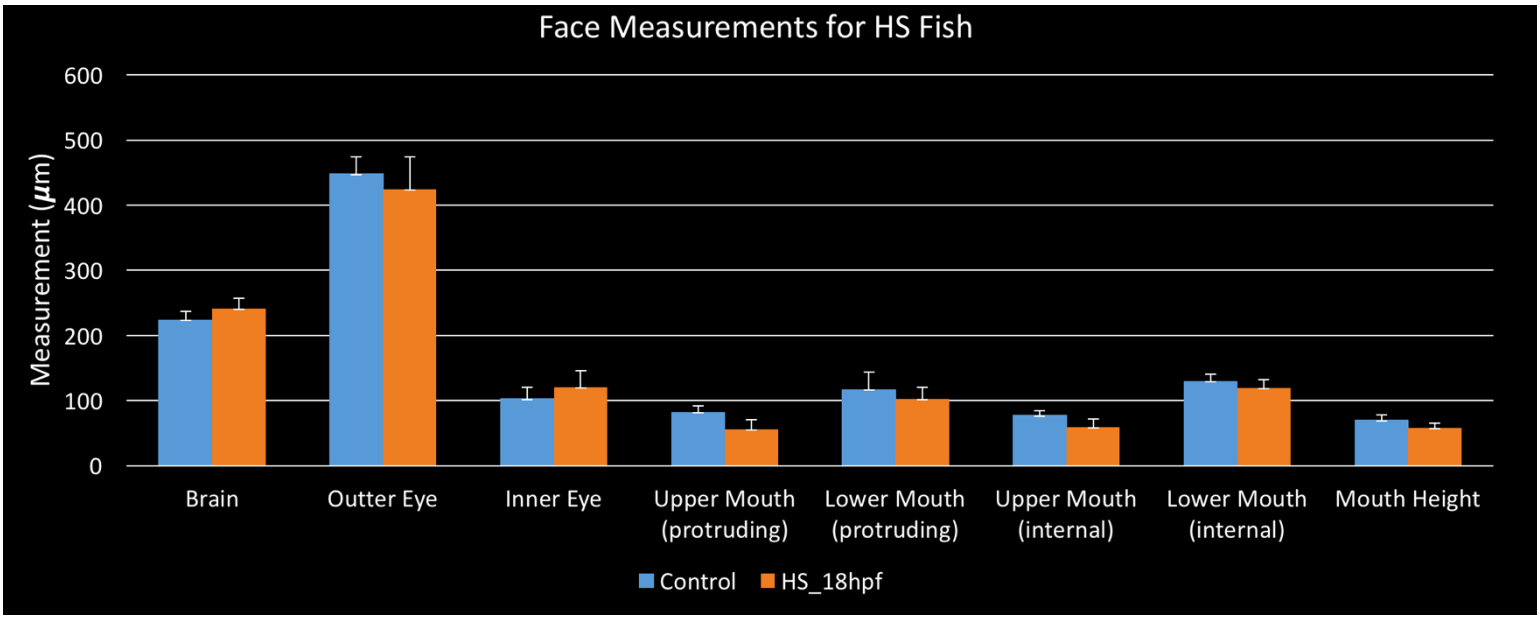

Figure 10. Measurement outcomes after fish were shocked at 40°C for 30 minutes at 18hpf. Measurements of the face were performed with heat shock positive and control fish. Each bar represents the average measurement value for given treatment group and measurement category. Error bars represent the standard deviation within the given treatment group or control. Average measurements were compiled with a minimum n-value of 5. From this data it was determined that a difference existed in mouth height (top to bottom), the upper mouth when protruding and the internal upper mouth between heat shock and control fish. Other measurement categories did not have a significant difference between control and heat shock fish. Significant differences between measurements were seen between overall mouth height ($p = 0.0415$) and the internal / external measurements of the upper mouth ($p = 0.0455$ and $p = 0.0275$ respectively). Significance levels were tested using a t Test comparing control and heat shock measured fish faces.

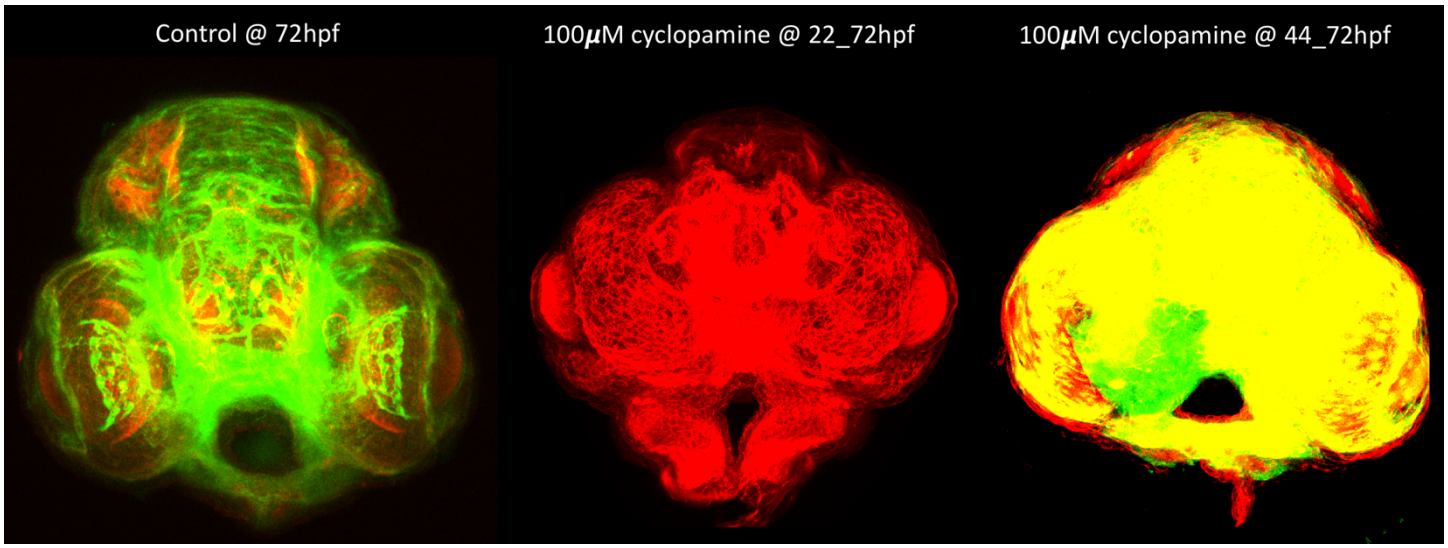

Figure 11. Drug treatments with Hh signaling smoothened antagonist, cyclopamine. Treatments with cyclopamine were at 22 and 44hpf, respectively. Once treated with cyclopamine, the fish were incubated at 28.5°C until 72hpf when they were treated with 4% PFA and prepared for imaging. All fish were Tg(*Fli1:GFP)* fish counter-stained with Rhodamine Phalloidin after being fixed in 4% PFA. All facial images are maximal intensity projections (MIPs) that include all sections of z-stack using confocal microscopy. Facial morphology disruptions were prevalent at both 22 and 44hpf, although the 22hpf treatment time resulted in a more severe phenotype.

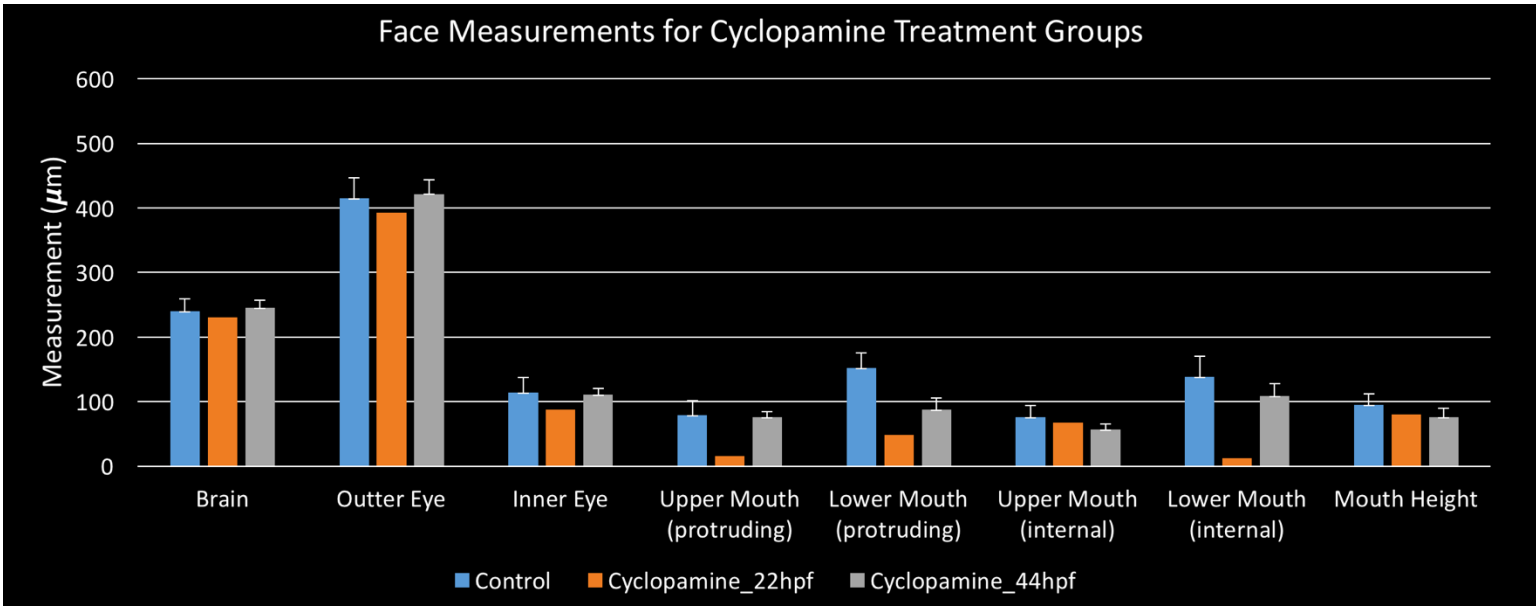

Figure 12. Measurement outcomes after treatment with Smoothened antagonist, Cyclopamine. Measurements of the face were performed with control, 22 and 44hpf treatment group fish. Average measurements were compiled with a minimum n-value of 5 and compared across control and treatment fish. Each bar represents the average measurement value for given treatment group and measurement category. Error bars represent the standard deviation within the given treatment group or control. From this data it was determined that there was a difference between 44hpf treated fish and control fish in mouth height, width of the lower protruding mouth and width of the lower internal mouth. While statistical difference couldn't be determined for the 22hpf treatment group, an obvious discrepancy exists between the upper protruding mouth size and lower internal mouth size. Significant differences between measurements were seen in the lower mouth external measurement ($p = 0.0043$) and the upper mouth internal measurement ($p = 0.0476$). Significance levels were tested using a t Test comparing control and cyclopamine treated fish face metrics.

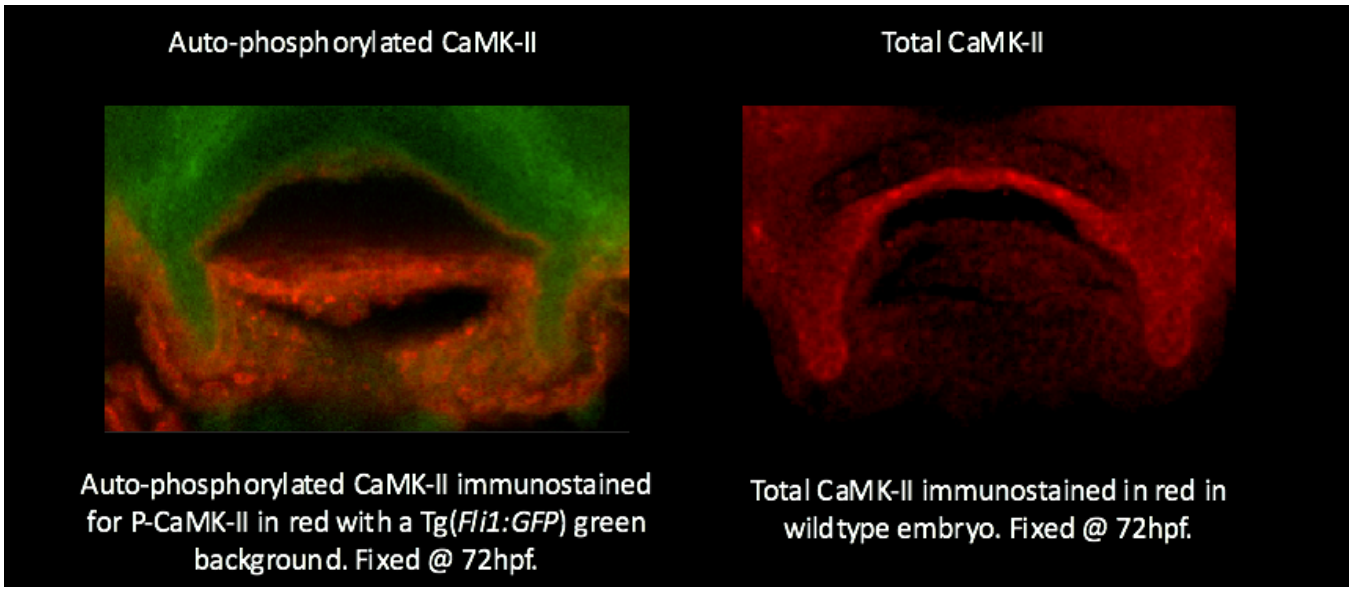

Figure 13. CaMK-II antibody staining. Immunolocalization using anti-phosphorylated CaMK-II (anti-P-CaMK-II; phosphorylated at Thr^{287}), and total CaMK-II. Immunostained for P-CaMK-II in Tg(*Fli1:GFP*) embryos and Immunostained for total CaMK-II in wildtype embryos. Embryos were fixed, stained and imaged at 72hpf. P-CaMK-II can be seen around the edge of the opening of the mouth on the image to the left and total CaMK-II can also be seen on the boundary of the perforated fish mouth on the right.

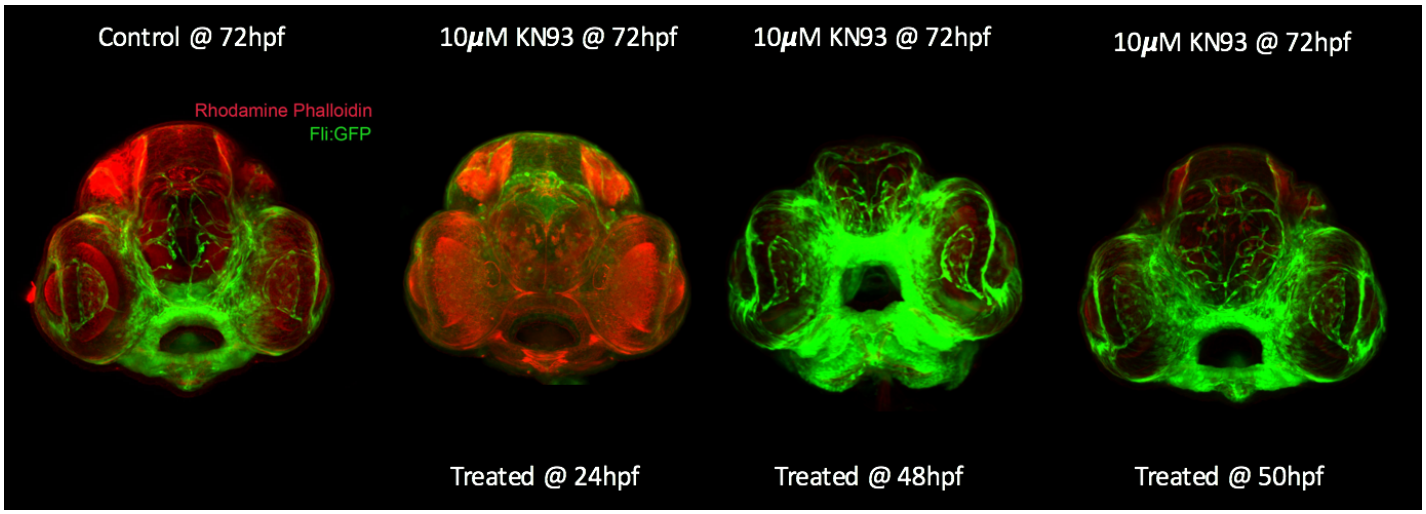

Figure 14. Drug treatments with KN93, a calmodulin binding site antagonist of CaMK-II. Treatments with KN93 were at 24, 48 and 50hpf, respectively. Once treated with KN93, the fish were incubated at 28.5°C until 72hpf when they were treated with 4% PFA and prepared for imaging. All fish were Tg(*Fli1:GFP)* fish counter-stained with Rhodamine Phalloidin after being fixed in 4% PFA. All facial images are maximal intensity projections (MIPs) that include all sections of z-stack using confocal microscopy. Facial morphology disruptions were seen to be primarily at 48hpf, with a box-mouthed phenotype having prevalence.

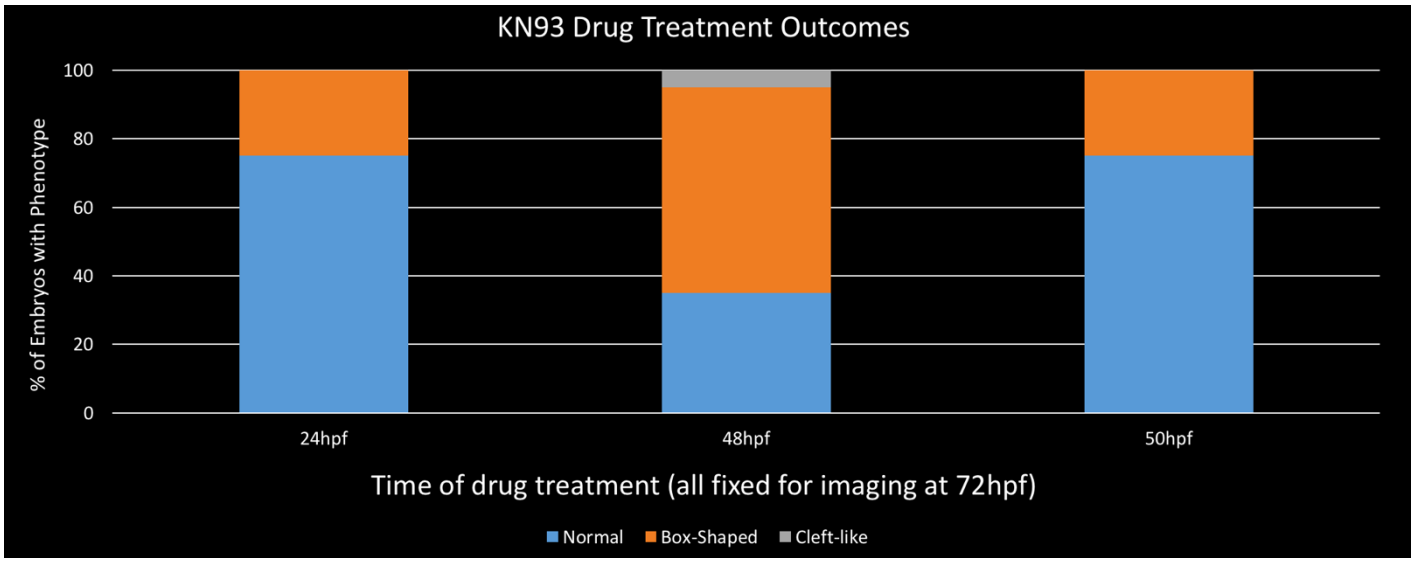

Figure 15. Drug treatment outcomes with KN93, a calmodulin binding site antagonist of CaMK-II. Treatments were at 24, 48, and 50hpf, respectively. Once treated with KN93, the fish were incubated at 28.5°C until 72hpf when they were treated with 4% PFA and prepared for imaging. Bars represent the percentage of fish with phenotypic changes to mouth morphology, indicated as being phenotypically normal (blue), box-shaped (orange) or cleft-like (grey). Oddly, it was concluded that KN93 treatment caused the most significant changes to facial development when treated at a later time point (48hpf). Treatments at both 24 and 50hpf resulted in subtle changes to head morphology but the most severe phenotype seen was a box-like mouth.

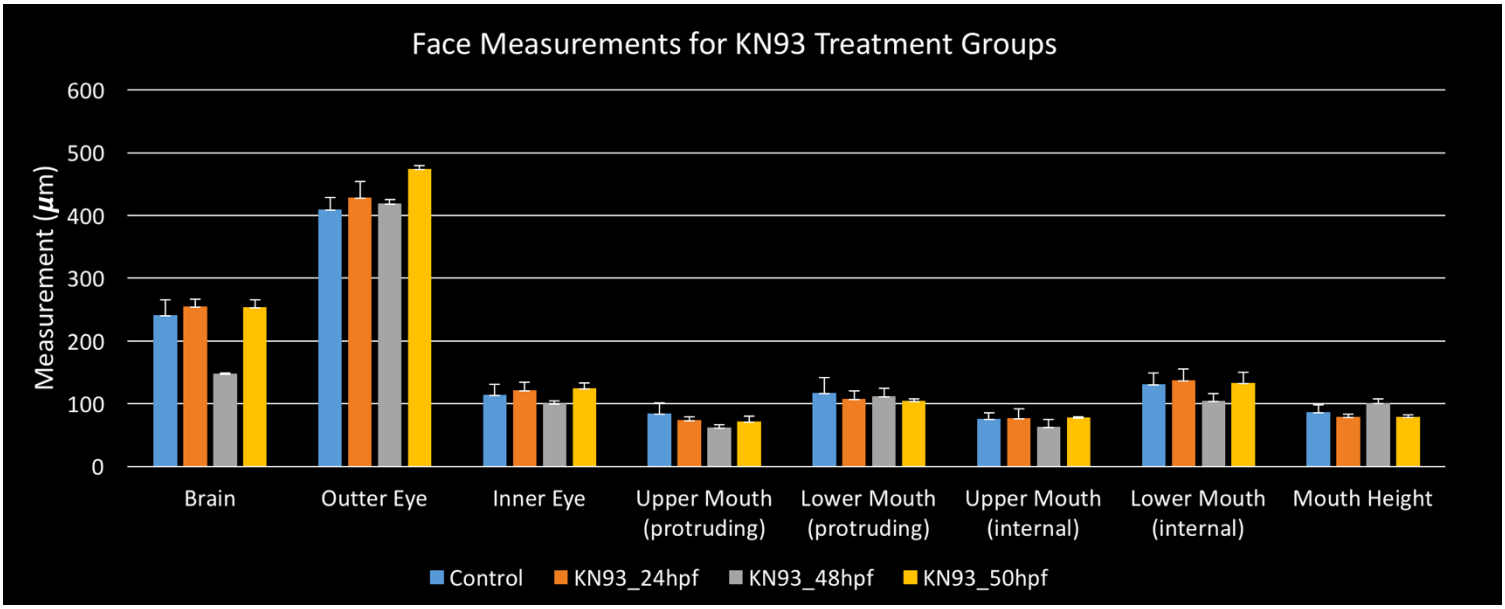

Figure 16. Measurement outcomes after treatment with calmodulin binding antagonist of CaMK-II, KN93. Measurements of the face were performed with control, 24, 48 and 50hpf treatment group fish. Average measurements were compiled with a minimum n-value of 5 and compared across control and treatment fish. Each bar represents the average measurement value for given treatment group and measurement category. Error bars represent the standard deviation within the given treatment group or control. From this data it was determined that there was a difference between 24hpf treated fish and control fish in mouth height (top to bottom). Furthermore, there was a difference seen between 48hpf treated fish and control fish in brain size and width of the mouth (both upper and lower) internally. The most significant measurement difference ($p = 0.0068$) was seen in 48hpf KN93 brain size. Significance levels were tested using a t Test comparing control and KN93 treated fish face metrics.

Discussion

When does the primary mouth form and what role does it have on secondary (adult) mouth formation? For *Xenopus*, the Dickinson lab (VCU Biology) has established some of the mechanisms and principals involved in the primary mouth's formation and eventual perforation to form the secondary mouth (reviewed in Dickinson 2016). From their discoveries and the findings of other craniofacial researchers we were able to seek out details of zebrafish primary mouth formation in a more informed manner. While the mechanism for perforation of the primary mouth in zebrafish seems to be different from that of *Xenopus* (Hamlett et al., 1996; Waterman and Kao, 1982), the primary mouth still serves the essential function of connecting the foregut to the external environment. In order to better understand this structure, we decided to investigate when the protruding mouth is first visible in zebrafish, as this is presumably directly after perforation and would serve as a marker for when primary mouth formation has come to pass. Initially there were concerns that the natural body curvature of *Danio* would prevent proper sectioning of the face and not allow for proper confocal imaging. Dispelling these concerns, we were able to create a series of time point images from 36-48hpf not only highlighting the orofacial developmental features but also validating our new imaging technique as one that is not as limited as one may have thought. From these results we were also able to confirm that *Danio* is capable of more rapid mouth formation than other model organisms currently being studied, a significant detail to consider when searching for novel sensitive time periods in craniofacial development. After seeing that the imaging technique was viable in establishing when the mouth is first formed in zebrafish, our next goal was to be able to recapitulate cleft-like phenotypes in zebrafish

and image them in this new forward facing manner. Surprisingly, most craniofacial research involving *Danio* has not been focused on the mouth, and instead is centered on bone, cartilage, and tooth growth. We suspect that the reason for this is the ease in which Alcian blue (cartilage stain) and Alizarin red staining (bone stain) can be used. That being said, key developmental pathways *have* been implicated in proper craniofacial / orofacial morphogenesis in zebrafish using these techniques (Mukhopadhyay 2008; Dickinson 2016; Swartz 2011; Liu et al., 2005). The first pathway we decided to investigate was the BMP signaling pathway. Treatment with the antagonist DMH1 did result in orofacial clefting, which we were able to capture qualitatively with our new imaging technique. Important to note is that our results echoed current literature in that our earlier treatment period (24hpf) produced the most severe orofacial defects, whereas our later treatment periods generally had no effect (42, 48hpf). We believe the reason for this is that the earlier treatment period (before 36hpf) results in reduced bmp2b and bmp4 expression, which has been shown to be essential in proliferation and survival of palatal precursors in zebrafish (Swartz 2011). In order to further examine the BMP signaling pathway, we decided to see what would happen if we had over-expression of BMP during development. Heat shocking at 18hpf resulted in severe craniofacial defects at 72hpf, statistical analysis showed a significant difference between mouth height and mouth width both externally and internally. We believe the 18hpf heat shock time may have had an effect on the tail-end of neural crest migration as neural crest cells are not fully resident to the face until 20hpf (Cusack et al. 2017). In conclusion, we were able to generate a cleft-like phenotype with both inhibition and overexpression of BMP signaling, reinforcing our imaging method as a valuable

way to qualitatively show the developmental role the BMP signaling pathways has. In order to explore other signaling pathways shown to be relevant in craniofacial development we decided to investigate the Hedgehog signaling pathway. Using the Hh signaling smoothened antagonist cyclopamine we were able to produce cleft like phenotypes at treatment times of both 22hpf and 44hpf. By treating at 22hpf and 44hpf we were able to recapitulate some of the results shown in previous literature in that treatments before 48hpf would result in clefting or at least loss of some jaw features (Wada 2005). We hypothesize that the treatment at 22hpf had an effect on NC migration whereas the treatment at 44hpf disrupted growth of cartilaginous features needed for proper palatogenesis. Previously in zebrafish craniofacial research a treatment time of 44hpf, after NC migration has occurred, would lead to solely investigating the cartilage and bone elements of the skull developing. However, with our imaging we were able to show that there is strength in being able to show the cleft phenotype in relation to the other data being collected (Figure 11). Lastly we decided to explore the role of CaMK-II in proper orofacial morphogenesis. By utilizing antibody Immunolocalization we were able to determine that both P-CaMK-II and total CaMK-II reside in the mouth region (Figure 13). From this we were able to determine that CaMK-II must have some role in mouth regulation otherwise expression would not be seen in the area. In order to elucidate what level of regulation CaMK-II may hold on the orofacial region we decided to use the calmodulin binding site antagonist of CaMK-II, KN93. Using KN93 to perturb CaMK-II signaling allowed for us to reveal whether the function CaMK-II had in the area was significant or mundane in nature. Out of the three treatment time points (24, 48, 50hpf) the 48hpf treatment time point had the most

severe morphological abnormalities. This is surprising however, as an earlier treatment time would usually result in more downstream consequences for craniofacial development. We believe KN93 function may weaken over time, indicating that the 48hpf treatment window may have been more significant and that the role CaMK-II plays on NC migration is not substantial (as earlier treatment times did not result in facial abnormalities). While evaluating measurement outcomes between KN93 treatment groups we noticed that brain size was one of the most dramatically changed values, indicating a potential role for KN93 on brain and skull formation. Establishing the primary mouth's formation in zebrafish, our ability to recapitulate phenotypes in a more visually captivating manner, and the speed in which we can establish novel mechanisms within developmental pathways shows the strength of *Danio* as a model for craniofacial research. Moving forward I feel as though this imaging technique should become standard as it is much more appealing than the current Alcian blue staining protocol used to show loss of mandibular components. While the technique may seem daunting initially it is not difficult to master and can be easily added to any current zebrafish orofacial research methodology to enhance their qualitative data. Quantitatively the potential for establishing morphometric landmarks using the forward facing zebrafish is promising. In conclusion the zebrafish is a vastly underrated model organism for studying mouth formation and development, something that can and should be changed moving forward.

Literature Cited

1. Abzhanov A, Protas M, Grant, B.R., Grant, P.R., Tabin, C.J. Bmp4 and Morphological Variation of Beaks in Darwin's Finches. *Science*. 2004:305:1462-1465.

2. Bayer KU, Lohler J, Schulman H, Harbers K. 1999. Developmental expression of the CaM kinase II isoforms: ubiquitous gamma- and delta-CaM kinase II are the early isoforms and most abundant in the developing nervous system. *Brain Res Mol Brain Res.* 70:147–154.

3. Braun A.P., Schulman H. 1995. The Multifunctional Calcium/Calmodulin-Dependent Protein Kinase: From Form to Function. *Annual Review of Physiology*. Vol. 57:417-445.

4. Briscoe J., Therond P.P., The mechanisms of Hedgehog signalling and its roles in development and diseaseNat. *Rev. Mol. Cell Biol*., 14 (2013), pp. 418–431.

5. Brocke L, Srinivasan M, Schulman H. 1995. Developmental and regional expression of multifunctional Ca^{2+}/calmodulin-dependent protein kinase isoforms in rat brain. *J Neurosci.* 15:6797– 6808.

6. Caspary T., Garcia-Garcia M.J., D. Huangfu, J.T. Eggenschwiler, M.R. Wyler, A.S. Rakeman, H.L. Alcorn, K.V. Anderson. Mouse Dispatched homolog1 is required for long-range, but not juxtacrine, Hh signaling. *Curr. Biol.*, 12 (2002), pp. 1628–1632.

7. Chiang C, Litingtung Y, Lee E, Young KE, Corden JL, Westphal H, Beachy PA. Cyclopia and defective axial patterning in mice lacking Sonic hedgehog gene function. *Nature*. 1996;383:407–413.

8. Cong W, Liu B, Liu S, et al. Implications of the Wnt5a/CaMKII Pathway in Retinoic Acid-Induced Myogenic Tongue Abnormalities of Developing Mice. *Scientific Reports*. 2014;4:6082.

9. Corbit K.C., P. Aanstad, V. Singla, A.R. Norman, D.Y. Stainier, J.F. Reiter Vertebrate smoothened functions at the primary cilium. *Nature*, 437 (2005), pp. 1018–1021.

10. Cordero D., R. Marcucio, D. Hu, W. Gaffield, M. Tapadia, J.A. Helms. Temporal perturbations in sonic hedgehog signaling elicit the spectrum of holoprosencephaly phenotypes. *J. Clin. Investig*., 114 (2004), pp. 485–494.

11. Creanga A., T.D. Glenn, R.K. Mann, A.M. Saunders, W.S. Talbot, P.A. Beachy Scube/You activity mediates release of dually lipid-modified Hedgehog signal in soluble form. *Genes Dev*., 26 (2012), pp. 1312–1325.

12. Dickinson A., H. Sive, Development of the primary mouth in *Xenopus laevis*, *Developmental Biology*, Volume 295, Issue 2, 15 July 2006, Pages 700-713.

13. Dickinson A., H. Sive, Positioning the extreme anterior in *Xenopus*: Cement gland, primary mouth and anterior pituitary, *Seminars in Cell & Developmental Biology*, Volume 18, Issue 4, August 2007, Pages 525-533.

14. Dickinson A., Using frogs faces to dissect the mechanisms underlying human orofacial defects, *Seminars in Cell & Developmental Biology*, Volume 51, March 2016, Pages 54-63.

15. Dickinson A., Sive H., The Wnt antagonists Frzb-1 and Crescent locally regulate basement membrane dissolution in the developing primary mouth. *Development (Cambridge, England)*. 2009;136(7):1071-1081.

16. Easley CA, Faison MO, Kirsch TL, Lee JA, Seward ME, Tombes RM. Laminin activates CaMK-II to stabilize the nascent embryonic axons. 2006. *Brain Res,* 1092:59-68.

17. Eberhart JK, Swartz ME, Crump JG, Kimmel CB. Early Hedgehog signaling from neural to oral epithelium organizes anterior craniofacial development. *Development*. 2006;133:1069–1077.

18. Gallea S, Lallemand F, Atfi A, Rawadi G, Ramez V, Spinella-Jaegle S, Kawai S, Faucheu C, Huet L, Baron R, Roman-Roman S. Activation of mitogen-activated protein kinase cascades is involved in regulation of bone morphogenetic protein-2-induced osteoblast differentiation in pluripotent C2C12 cells. *Bone*. 2001;28:491–498.

19. Goodrich L.V., R.L. Johnson, L. Milenkovic, J.A. McMahon, M.P. Scott Conservation of the hedgehog/patched signaling pathway from flies to mice: induction of a mouse patched gene by Hedgehog. *Genes Dev*., 10 (1996), pp. 301–312.

20. Gritli-Linde A., P. Lewis, A.P. McMahon, A. Linde The whereabouts of a morphogen: direct evidence for short- and graded long-range activity of hedgehog signaling peptides *Dev. Biol*., 236 (2001), pp. 364–386.

21. Guilherme M. Xavier, Maisa Seppala, William Barrell, Anahid A. Birjandi, Finn Geoghegan, Martyn T. Cobourne, Hedgehog receptor function during craniofacial development, *Developmental Biology*, Volume 415, Issue 2, 15 July 2016, Pages 198-215.

22. Hamlett WC, Schwartz FJ, Schmeinda R, Cuevas E. Anatomy, histology, and development of the cardiac valvular system in elasmobranchs. *Journal of Experimental Zoology.* 1996;275:83–94.

23. Haycraft C.J., B. Banizs, Y. Aydin-Son, Q. Zhang, E.J. Michaud, B.K. Yoder. Gli2 and Gli3 localize to cilia and require the intraflagellar transport protein polaris for processing and function. *PLoS Genet*., 1 (2005), p. e53.

24. Hogan BL. Bone morphogenetic proteins in development. *Curr Opin Genet Dev*. 1996a;6:432–438.

25. Hogan BLM. Bone morphogenetic proteins: Multifunctional regulators of vertebrate development. *Genes Dev*. 1996b;10:1580–1594.

26. Hollnagel A, Oehlmann V, Heymer J, Ruther U, Nordheim A. Id genes are direct targets of bone morphogenetic protein induction in embryonic stem cells. *J Biol Chem*. 1999;274:19838–19845.

27. Hu D, Helms JA. The role of sonic hedgehog in normal and abnormal craniofacial morphogenesis. *Development.* 1999;126:4873–4884.

28. Hu D., R.S. Marcucio, J.A. Helms. A zone of frontonasal ectoderm regulates patterning and growth in the face. *Development,* 130 (2003), pp. 1749–1758.

29. Hu D., R.S. Marcucio. A SHH-responsive signaling center in the forebrain regulates craniofacial morphogenesis via the facial ectoderm. *Development*, 136 (2009), pp. 107–116.

30. Hudmon A, Schulman H. 2002. Neuronal Ca^{2+}/Calmodulin-dependent protein kinase II: the role of structure and autoregulation in cellular function. *Annu Rev Biochem* 71:473–510.

31. Kawakami T., T. Kawcak, Y.J. Li, W. Zhang, Y. Hu, P.T. Chuang Mouse dispatched mutants fail to distribute hedgehog proteins and are defective in hedgehog signaling. *Development*, 129 (2002), pp. 5753–5765.

32. Kawakami K, Koga A, Hori H, Shima A. Excision of the *Tol2* transposable element of the medaka fish, *Oryzias latipes*, in zebrafish, *Danio rerio*. *Gene*. 1998;225:17–22.

33. Kimmel C.B., W.W. Ballard, S.R. Kimmel, B. Ullmann, T.F. Schilling. Stages of embryonic development of the zebrafish. *Dev. Dyn.*, 203 (1995), pp. 253–310.

34. Kishigami S, Yoshikawa S, Castranio T, Okazaki K, Furuta Y, Mishina Y. BMP signaling through ACVRI is required for left-right patterning in the early mouse embryo. *Dev Biol*. 2004;276:185–193.

35. Kishigami S, Mishina Y. Bmp signaling and early embryonic patterning. *Cytokine Growth Factor Rev*. 2005;16:265–278.

36. Korchynskyi O, Dechering KJ, Sijbers AM, Olijve W, ten Dijke P. Gene array analysis of bone morphogenetic protein type I receptor-induced osteoblast differentiation. *J Bone Miner Res*. 2003;18:1177–1185.

37. Lan Y, Ryan RC, Zhang Z, Bullard SA, Bush JO, Maltby KM, Lidral AC, Jiang R. Expression of Wnt9b and activation of canonical Wnt signaling during midfacial morphogenesis in mice. *Dev Dyn*. 2006;235:1448–1454

38. Lawson ND, Weinstein BM. In vivo imaging of embryonic vascular development using transgenic zebrafish. *Dev Biol*. 2002;248:307–318.

39. Lee CT, Risom T, Strauss WM. MicroRNAs in mammalian development. *Birth Defects Res C Embryo Today*. 2006;78:129–139.

40. Liu W, Sun X, Braut A, et al. Distinct functions for Bmp signaling in lip and palate fusion in mice. *Development*. 2005;132:1453–1461.

41. Lyons KM, Pelton RW, Hogan BL. Organogenesis and pattern formation in the mouse: RNA distribution patterns suggest a role for bone morphogenetic protein-2A (BMP-2A) *Development*. 1990;109:833–844.

42. Ma Y., A. Erkner, R. Gong, S. Yao, J. Taipale, K. Basler, P.A. Beachy. Hedgehog-mediated patterning of the mammalian embryo requires transporter-like function of dispatched. *Cell*, 111 (2002), pp. 63–75.

43. Macias-Silva M, Hoodless PA, Tang SJ, Buchwald M, Wrana JL. Specific activation of Smad1 signaling pathways by the BMP7 type I receptor, ALK2. *J Biol Chem*. 1998;273:25628–36.

44. Miller, C. T., Schilling, T. F., Lee, K.-H., Parker, J. and Kimmel, C. B. (2000). Sucker encodes a zebrafish endothelin-1 required for ventral pharyngeal arch development. Development 127,3815 -3828.

45. Mukhopadhyay P, Webb C, Warner D, et al. BMP signaling dynamics in embryonic orofacial tissue. *J Cell Physiol*. 2008;216:771–779.

46. Noden DM. The control of avian cephalic neural crest cytodifferentiation. I. Skeletal and connective tissues. *Dev Biol.* 1978. 67, 296–312.

47. Noden DM. The role of the neural crest in patterning of avian cranial skeletal, connective, and muscle tissues. *Devel Biol. 1983.* 96, 144–165.

48. Noden DM. Interactions and fates of avian craniofacial mesenchyme. *Development. 1988.* **103**, 121–140.

49. Nohe A, Keating E, Knaus P, Petersen NO. Signal transduction of bone morphogenetic protein receptors. *Cell Signal*. 2004;16:291–299.

50. Ogata T, Wozney JM, Benezra R, Noda M. Bone morphogenetic protein 2 transiently enhances expression of a gene, Id (inhibitor of differentiation), encoding a helix-loop-helix molecule in osteoblast-like cells. *Proc Natl Acad Sci USA*. 1993;90:9219–9222.

51. Pepinsky R.B., Zeng C., Wen D., Rayhorn P., Baker D.P., Williams K.P., Bixler S.A., Ambrose C.M., Garber E.A., Miatkowski K., Taylor F.R., Wang E.A., Galdes A. Identification of a palmitic acid-modified form of human Sonic hedgehog *J. Biol. Chem*., 273 (1998), pp. 14037–14045.

52. Petrova R., Joyner A.L., Roles for Hedgehog signaling in adult organ homeostasis and repair. *Development*, 141 (2014), pp. 3445–3457.

53. Petryk A, Graf D, Marcucio R. Holoprosencephaly: signaling interactions between the brain and the face, the environment and the genes, and the phenotypic variability in animal models and humans. *Wiley Interdiscip Rev Dev Biol*. 2015;4:17–32.

54. Porter J.A., D.P. von Kessler, S.C. Ekker, K.E. Young, J.J. Lee, K. Moses, P.A. Beachy

55. The product of hedgehog autoproteolytic cleavage active in local and long-range signaling. *Nature*, 374 (1995), pp. 363–366.

56. Rohatgi R., L. Milenkovic, M.P. Scott Patched1 regulates hedgehog signaling at the primary cilium. *Science*, 317 (2007), pp. 372–376.

57. Roessler E, Belloni E, Gaudenz K, Jay P, Berta P, Scherer SW, Tsui LC, Muenke M. Mutations in the human Sonic Hedgehog gene cause holoprosencephaly. *Nat Genet*. 1996;14:357–360.

58. Rothschild SC, Lister JA, Tombes RM. 2007. Differential expression of CaMK-II genes during early zebrafish embryogenesis. *Dev Dyn.* 236:295–305.

59. Rothschild SC, L. Francescatto, I.A. Drummond, R.M. Tombes. CaMK-II is a PKD2 target that promotes pronephric kidney development and stabilizes cilia. *Development*, 138 (2011), pp. 3387–3397.

60. Rothschild SC, Lahvic J, Francescatto L, McLeod J, Burgess SM, Tombes R.M., CaMK-II activation is essential for zebrafish inner ear development and acts through Delta–Notch signaling, *Developmental Biology*, Volume 381, Issue 1, 1 September 2013, Pages 179-188.

61. Sabbagh HJ, Innes NP, Sallout BI, et al. Birth prevalence of non-syndromic orofacial clefts in Saudi Arabia and the effects of parental consanguinity. *Saudi Medical Journal*. 2015;36(9):1076-1083.

62. Soderling T. R., Chang B., Brickey D. Cellular signaling through multifunctional Ca^{2+}/calmodulin-dependent protein kinase II. *J. Biol. Chem*. 2001;276:3719–3722.

63. Soukup V, Horácek I, Cerny R. Development and evolution of the vertebrate primary mouth. *Journal of Anatomy*. 2013;222(1):79-99.

64. Swartz ME, Sheehan-Rooney K, Dixon MJ, Eberhart JK. Examination of a palatogenic gene program in zebrafish. *Dev Dyn*. 2011;240:2204–20.

65. Schworer CM, Rothblum LI, Thekkumkara TJ, Singer HA. 1993. Identification of novel isoforms of the delta Subunit of Ca^{2+}/ calmodulin-dependent protein kinase II. *J Biol Chem* 268:14443–14449.

66. Tabler JM, Bolger TG, Wallingford J, Liu KJ. Hedgehog activity controls opening of the primary mouth. *Developmental biology*. 2014;396(1):1-7.

67. Tobimatsu T, Fujisawa H. 1989. Tissue specific expression of four types of rat calmodulin-dependent protein kinase II mRNAs. *J Biol Chem* 264:17907–17912.

68. Tombes RM, Mikkelsen RB, Jarvis WD, Grant S. 1999. Down regulation of delta CaM kinase II in human tumor cells. *Biochim Biophys Acta.* 1452:1–11.

69. Tombes RM, Faison MO, Turbeville JM. Organization and evolution of multifunctional Ca(2+)/CaM-dependent protein kinase genes. *Gene*. 2003;322:17–31.

70. Tukachinsky H., R.P. Kuzmickas, C.Y. Jao, J. Liu, A. Salic Dispatched and scube mediate the efficient secretion of the cholesterol-modified hedgehog ligand. *Cell Rep*., 2 (2012), pp. 308–320.

71. Verma S., Geller K., Persistent buccopharyngeal membrane: Report of a case and review of the literature, *International Journal of Pediatric Otorhinolaryngology*, Volume 73, Issue 6, June 2009, Pages 877-880.

72. von Bubnoff A, Cho KW. Intracellular BMP signaling regulation in vertebrates: Pathway or network? *Dev Biol*. 2001;239:1–14.

73. Wada, N., Javidan, Y., Nelson, S., Carney, T. J., Kelsh, R. N. and Schilling, T. F. (2005). Hedgehog signaling is required for cranial neural crest morphogenesis and chondrogenesis at the midline in the zebrafish skull. *Development*. 132, 3977-3988.

74. Waterman RE. Ultrastructure of oral (buccopharyngeal) membrane formation and rupture in the hamster embryo. *Dev Biol*. 1977;58:219–229.

75. Waterman RE. Formation and perforation of closing plates in the chick embryo. *Anat Rec*. 1985;211:450–457.

76. Waterman RE, Kao R. Formation of the mouth opening in the zebrafish embryo. In: O'Hare AMF, editor. *Scanning Electron Microscopy*/1982/III. Chicago, IL: SEM; 1982. pp. 1249–1257.

77. Wozney JM, Rosen V, Celeste AJ, Mitsock LM, Whitters MJ, Kriz RW, Hewick RM, Wang EA. Novel regulators of bone formation: Molecular clones and activities. *Science*. 1988;242:1528–1534.

78. Yamamoto N, Akiyama S, Katagiri T, Namiki M, Kurokawa T, Suda T. Smad1 and smad5 act downstream of intracellular signalings of BMP-2 that inhibits myogenic differentiation and induces osteoblast differentiation in C2C12 myoblasts. *Biochem Biophys Res Commun.* 1997;238:574–580.

79. Zhang Z, Song Y, Zhao X, Zhang X, Fermin C, Chen Y. Rescue of cleft palate in Msx1-deficient mice by transgenic Bmp4 reveals a network of BMP and Shh signaling in the regulation of mammalian palatogenesis. *Development*. 2002;129:4135–4146.

80. Zhang X.M., M. Ramalho-Santos, A.P. McMahon Smoothened mutants reveal redundant roles for Shh and Ihh signaling including regulation of L/R symmetry by the mouse node. *Cell*, 106 (2001), pp. 781–792.

81. Zhao M, Xiao G, Berry JE, Franceschi RT, Reddi A, Somerman MJ. Bone morphogenetic protein 2 induces dental follicle cells to differentiate toward a cementoblast/osteoblast phenotype. *J Bone Miner Res*. 2002;17:1441–1451.

VITA

Kevin Amir Ghaffari was born on February 2nd, 1994 in Newport News, VA. He received his B.S. in Interdisciplinary Science in May 2015 from Virginia Commonwealth University.